ABSTRACT

WARM UNIT STAND ASSEMBLY AND TESTING FOR PROTON IMPROVEMENT PROJECT II

Chris English, MS
Department of Mechanical Engineering
Northern Illinois University, 2024
Nicholas Pohlman, Director

The Proton Improvement Project II (PIP II), situated at Fermilab, signifies a critical advancement in the realm of high-energy physics. PIP II, a linear accelerator renovation endeavor, aspires to double the output of the existing proton beam, reinforcing Fermilab' s position as a vanguard in this field. The proton beam's creation involves a series of high-frequency cryomodules, necessitating environmental temperature arrays of magnets and vacuum pumps henceforth described as 'Warm Units.' The Warm Units include design features of : 1. insertion between the cryomodules, 2. multi-stage adjustments in six degrees of freedom to ensure precise beam alignment; 3. Natural frequency modes that avoid specified ranges. In adherence to Fermilab' s stringent safety standards, comprehensive testing procedures are slated to validate the Warm Units' capacity to simultaneously achieve local alignment adjustments while averting low-frequency oscillation less than 15 Hertz. The testing regimen will scrutinize the Warm Units' alignment adjustment capabilities and their resilience against low-frequency oscillations, with an overarching objective of satisfying the Final Design Review criteria specific to the PIP II initiative. This project works to furnish technicians responsible for the assembly of Warm Units with a comprehensive guide for successful installation, concurrently documenting any requisite design modifications essential for achieving a real-world configuration.

NORTHERN ILLINOIS UNIVERSITY

DEKALB, ILLINOIS

MAY 2024

WARM UNIT STAND ASSEMBLY AND TESTING FOR PROTON IMPROVEMENT PROJECT II

BY

CHRISTOPHER A. ENGLISH

A THESIS SUBMITTED TO THE GRADUATE SCHOOL

IN PARTIAL FULFILLMENT OF THE REQUIREMENTS

FOR THE DEGREE

MASTER OF SCIENCE

DEPARTMENT OF MECHANICAL ENGINEERING

Thesis Director:

Nicholas Pohlman

ACKNOWLEDGMENTS

Thank you to Curtis Baffes (Mechanical Engineering Manager), Kyle Kendrioza (Mechanical Engineer), and Nicholas Pohlman (PhD) for their support and guidance throughout the project and research. Their help in defining constraints, safety concerns, and parameters, as well as previous work done, is what made the design possible. Special thanks to Fermilab and its various staff for helping facilitate research and assisting with quality assurance for the design. an especial thanks must go to Adam Wixson and Jeremiah Holzbauer for providing the code needed to scaffold to successfully parse the data. Lastly, my heartfelt thanks go out to my parents and friends, whose unwavering support and encouragement have been a constant source of motivation throughout this journey.

Table of Contents

LIST OF TABLES

LIST OF FIGURES

DEFINITIONS

Warm Unit – Instrumentation package comprised of vacuum ion pump, 2 dipole corrector magnets, and 2 quadrupole refocusing magnets

Corrector package – Combination of dipole corrector and quadrupole refocusing magnets

WURM – Warm Unit Rod Movement

FESHM – Fermilab Environment and Safety Hazards Manual

HB-650 - High-intensity beam, High Beta 650 MHz cryomodule

SSR-1 – Low-intensity single-spoke resonator cryomodule

RF Cavity – Radio Frequency cavity

Cryomodule – Accelerator instrumentation responsible for accelerating proton beam

PDR – Preliminary Design Review

PIP-II – Proton Improvement Project II

LINAC – Linear Accelerator

LEBT – Low Energy Beam Transfer

MEBT – Medium Energy Beam Transfer

DOF – Degrees of freedom

ORCA – Optimized Retaining Cryomodule Adjusters

Rafts – Rigid platforms that the turnbuckles of the WURM stand adjust

NX – 3D modeling software from Siemens

ANSYS – Finite element software used for analysis

1. INTRODUCTION

1.1 BACKGROUND

Fermilab has provided invaluable experimental data to the scientific community at large due to its large-scale particle accelerator. However the current particle accelerator is dated, and with the advent of the Large Hadron Collider at CERN, the equipment needs to be updated to stay in relevancy. PIP-II (Proton Improvement Project II) is a project that aims to replace the existing equipment in the Linac (Linear Accelerator shown in Figure 1).

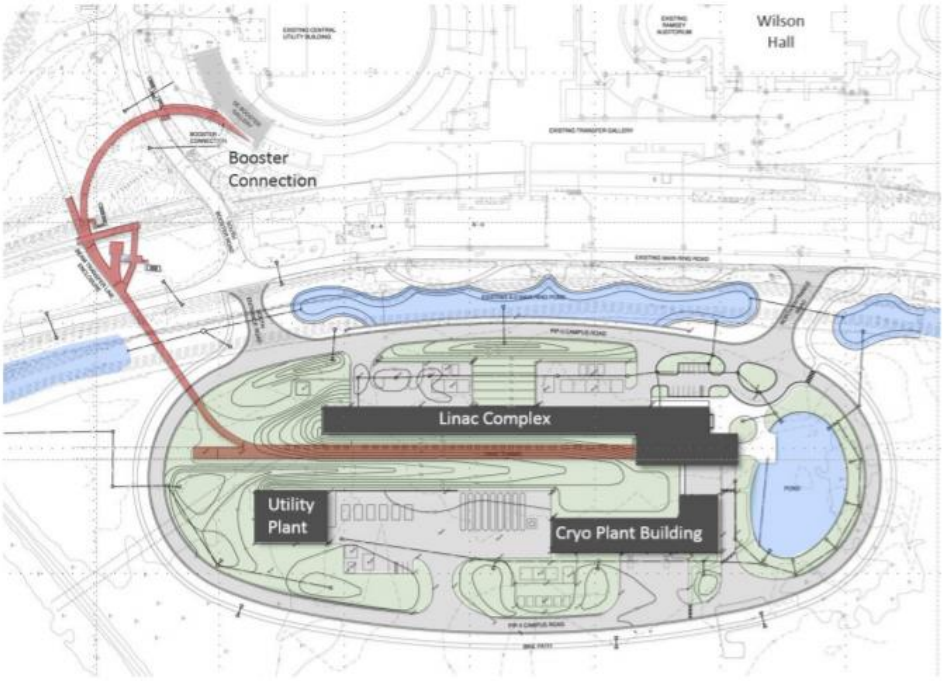

Figure 1: Map View of Linac [1]

Currently, Fermilab boasts the most intense proton beam in the world. The upgrades from PIP-II will ensure the beam will remain the most intense by doubling the intensity to 800 MeV [1]. In fact, several parameters are due to be upgraded, such as reduction in beam current, beam power, and pulse length. The various desired upgrades from PIP II are shown in Table 1.

Performance Parameter	PIP	PIP-II	Unit
Linac Beam Energy	400	800	MeV
Linac Beam Current (chopped)	25	2	mA
Linac Pulse Length	0.03	0.54	ms
Linac Pulse Repetition Rate	15	20	Hz
Linac Upgrade Potential	N/A	CW	
Booster Protons per Pulse (extracted)	4.2	6.5	10^{12}
Booster Pulse Repetition Rate	15	20	Hz
Booster Beam Power @ 8 GeV	80	166	kW
8 GeV Beam Power to LBNF	N/A	83-142*	kW
Beam Power to 8 GeV Program	30	83-24*	kW
Main Injector Protons per Pulse (extracted)	4.9	7.5	10^{13}
Main Injector Cycle Time @ 120 GeV	1.33	1.2	sec
Main Injector Cycle Time @ 60 GeV	N/A	0.7	sec
Beam Power @ 60 GeV	N/A	1	MW
Beam Power @ 120 GeV	0.7	>1	MW
Upgrade Potential @ 80-120 GeV	N/A	2.4	MW
* the first number refers to Main Injector operations at 120 GeV, second number to 60 GeV			

Table 1: Upgrades to Linac [1]

The components that make up the Linac are a series of low, medium, and high intensity cryomodules, and instrumentation packages with significantly higher relative temperature called warm units. The cryomodules contain a series chain of RF (radiofrequency) cavities that accelerate the proton beam, and the entire package is cooled to 2 K. An example low energy cryomodule (SSR1) is shown in Figure 2.

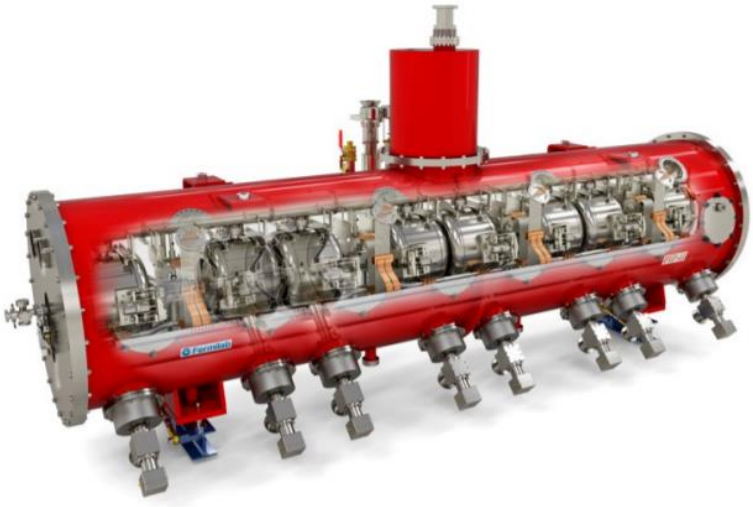

Figure 2: SSR1 Cryomodule [1]

There are 23 cryomodules in total in the Linac with multiple different configurations. The Linac is partitioned to different sections based on what stage of acceleration the proton beam is expected to experience. LEBT (low energy beam transfer) and MEBT (medium energy beam transfer) sections of the Linac dictate which type of cryomodule is used. The SSR1 cryomodule shown in Figure 3 for example, is placed in the LEBT section, while a HB-650 (high beta 650MHz) cryomodule is placed in the MEBT section.

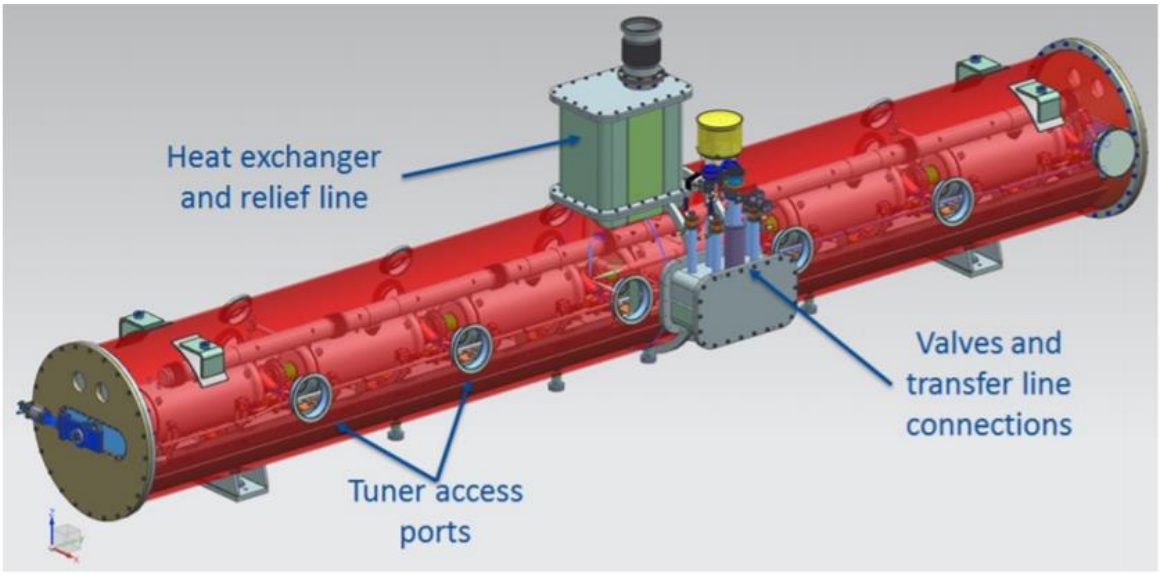

Figure 3: HB-650 Cryomodule [1]

The spacing in between the HB-650 cryomodules is where any correctional or monitoring instrumentation would be placed. Figure 4 shows the available space between the cryomodules of 1.3 m. Operating within this space is vital, as any components protruding past the envelope will interfere or damage components designed by other departments within Fermilab.

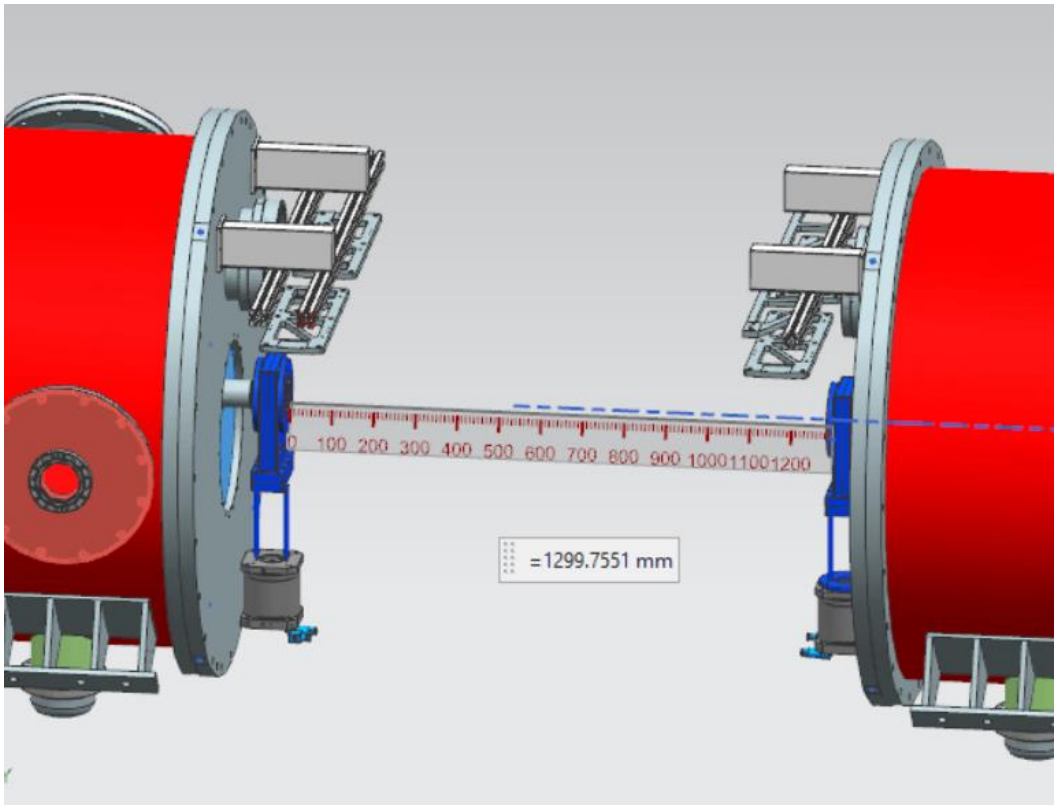

Figure 4: Spacing Between HB-650

Unfortunately, the proton beam diffuses during acceleration, and thus requires correction and refocusing in between each stage. Instrumentation packages called warm units are placed in between each cryomodule. These warm units ensure that the proton beam operates in vacuum and provide sufficient correction and refocusing before it is accelerated again. The reasoning for the name is that the instrumentation operates at room temperature. Figure 5 shows a warm unit which will sit in between two HB-650 cryomodules.

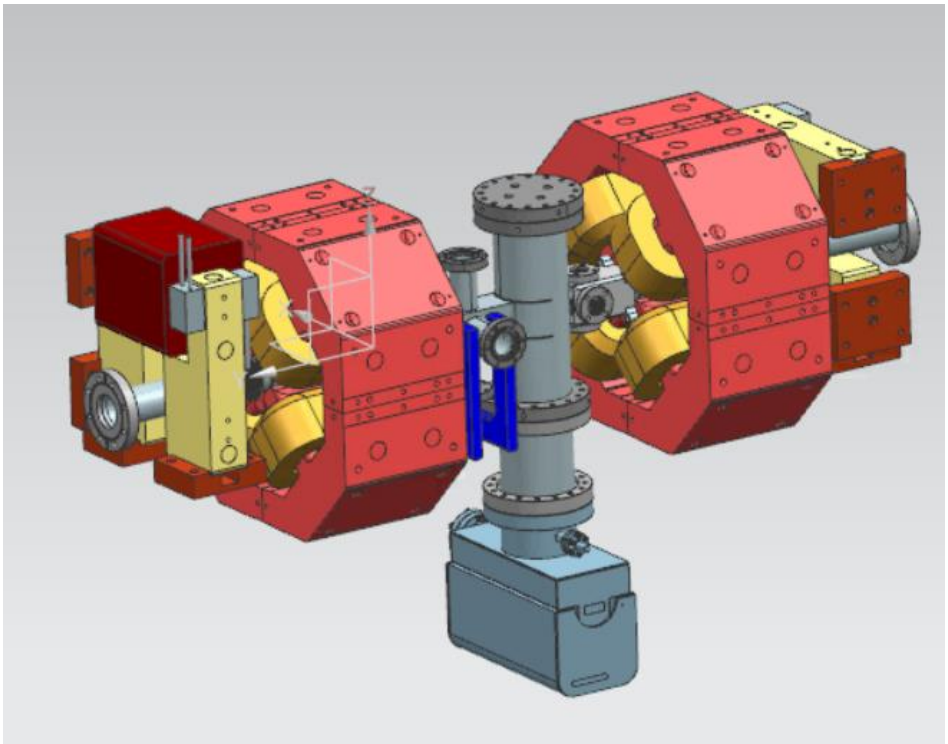

Figure 5: HB-650 Warm Unit

1.2 PURPOSE OF THE PROJECT

It is crucial to ensure that the warm unit instrumentation perfectly aligns with the proton beam. In an ideal scenario, all components will fit neatly together without the need for adjustment. However, there are always discrepancies between the ideal model and physical product: due to poor tolerances, or in this case, uneven flooring. The design dictates that the entire warm unit instrumentation package requires six DOF adjustments with a range of +/-30 mm. The warm units in between the HB-650 cryomodules contain two dipole-quad magnet packages. As such, each package requires its own six DOF of adjustment. The range of individual magnet package adjustment is +/- 15 mm. The beamline is 1.3 m from the floor. Not only does the warm unit need to align with the beamline, but it also has strict do-not-exceed envelopes shown in Figure 6. The envelopes ensure that the warm unit stays within 1.3 m along the beamline and includes any additional monitoring equipment added on in the future. A

physical structure is required to, position the warm unit in the proper location and orientation, provide the necessary adjustment, and properly support the weight in all orientations. The do-not-exceed values of warm unit instrumentation is 1100 kg total: 500 kg for each dipole-quad package and 100 kg for vacuum pump instrumentation and piping. It is imperative to subject the assembled structure to rigorous testing to ensure that it conforms to all criteria and specifications delineated during the design process.

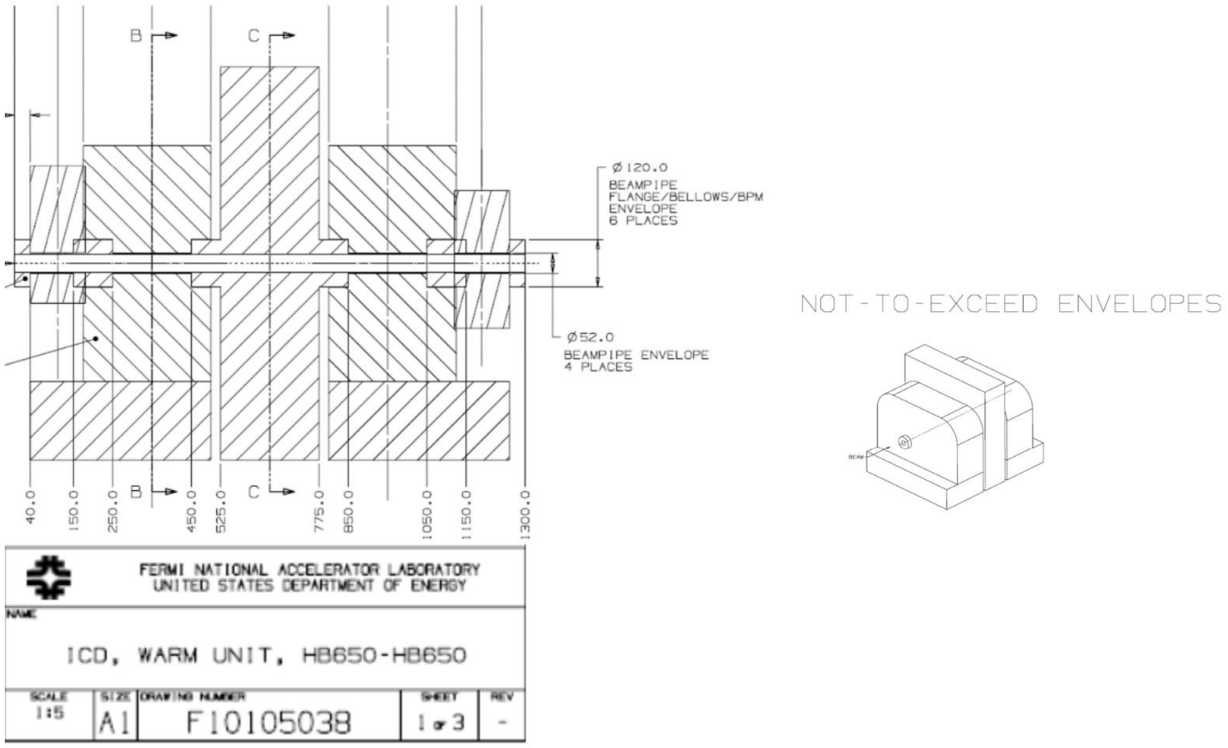

Figure 6: Dimensions of Do-Not-Exceed Envelopes

1.3 PREVIOUS WORK

Much of the study for beam physics and instrumentation requirements were set by the collaborative teams at Argonne National Laboratories, Bhabha Atomic Research Center, Fermi National Accelerator Laboratory, Raja Rammana Center for Advanced Technology, and Wroclaw University of Science and Technology [1]. Previous proposals concerning similar adjustments to the cryomodules were studied to understand how to engage in warm unit stand

design. Figure 7 shows the proposal for a 6 DOF adjustment solution for the cryomodule, affectionately named ORCA (circled in purple) [2]. The ORCA Stand is a two-part, floor-mounted solution with three adjustment rods with locking collars per part. It is capable of +/- 30 mm of adjustment. Three of the rods are oriented vertically, two rods are oriented laterally, and one rod runs along the beam axis. The configuration of adjustment rods ensures that the stand is kinematic. The stand locks in place unless adjusted.

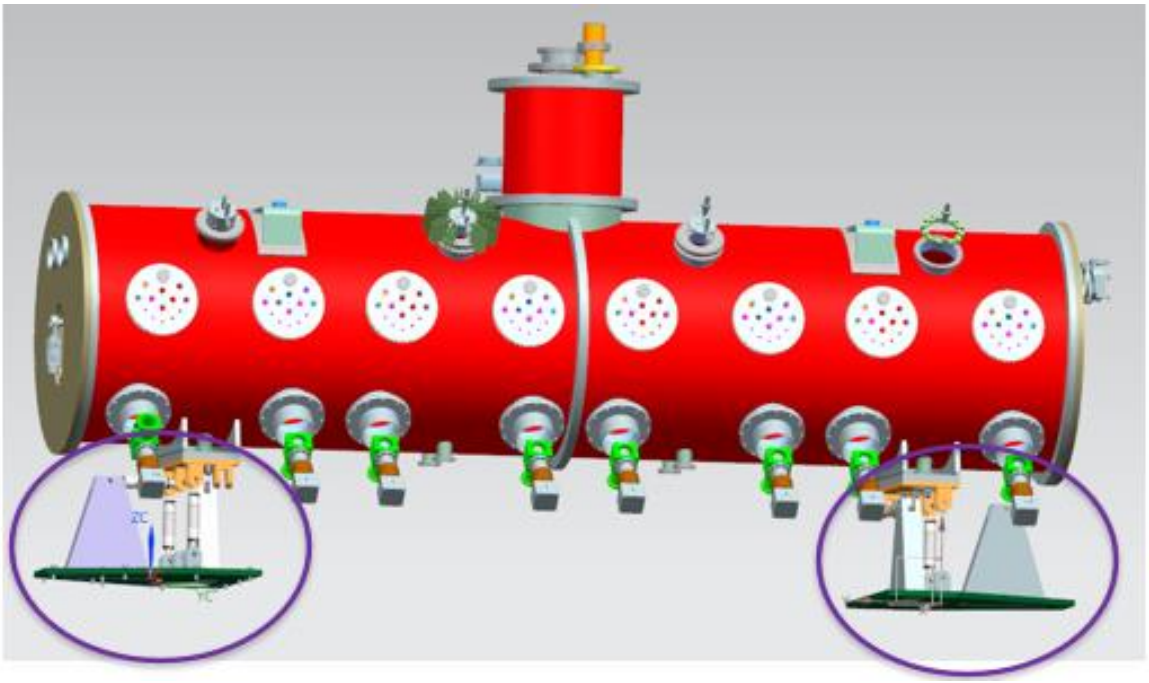

Figure 7: ORCA Cryomodule Adjustment Stand [2]

Figure 8 shows a closer look at the ORCA Stand [3]. The adjustment rods are shown with their locking collars in the locked position. The locking of the stand is critical, as the 14000 kg mass of the SSR1 cryomodule is a hazard if unsecure. Analysis was completed to ensure safe operation of the ORCA Stand in terms of weld stress, plate stress, cryomodule stress, and rod stress [4]. Since the analysis was deemed satisfactory, the design of the warm unit adjustment stand borrowed from ORCA. The following design owes much to the team that designed the

ORCA stand.

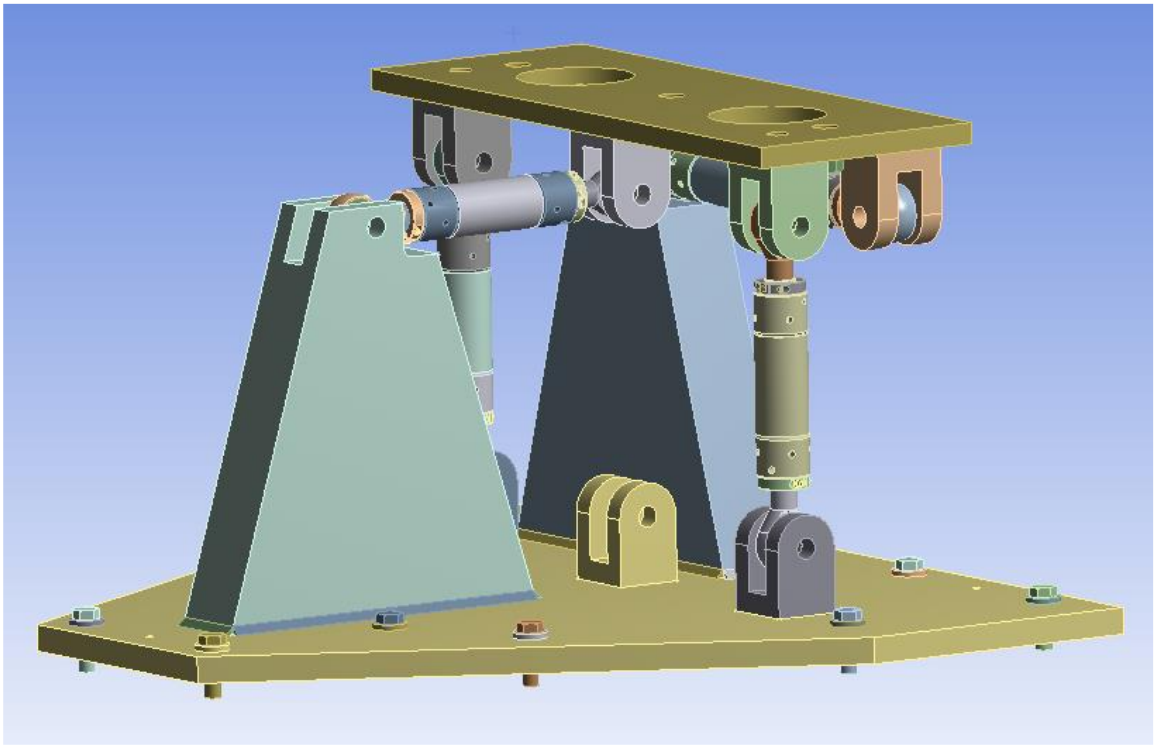

Figure 8: Close up of One Half of ORCA [3]

Within the context of ORCA, two distinct platforms were developed: one intended for the 325 MHz range and another for the 650 MHz range. Each platform features a six-degree-of-freedom mechanism, accommodating a quadrupole corrector magnet. The 650 MHz frame is designed to house two platforms, each supporting a different quadrupole, necessitating a total of 18 adjustable turnbuckles. This configuration enhances the system's adaptability, enabling it to address a wide range of scenarios.

Furthermore, the structural dynamics were thoroughly analyzed using ANSYS and MATLAB simulations, which helped identify various extremal modes and natural frequencies [5, 6]. These findings will significantly influence the test procedures for the structure, ensuring its robustness and performance under various operational conditions.

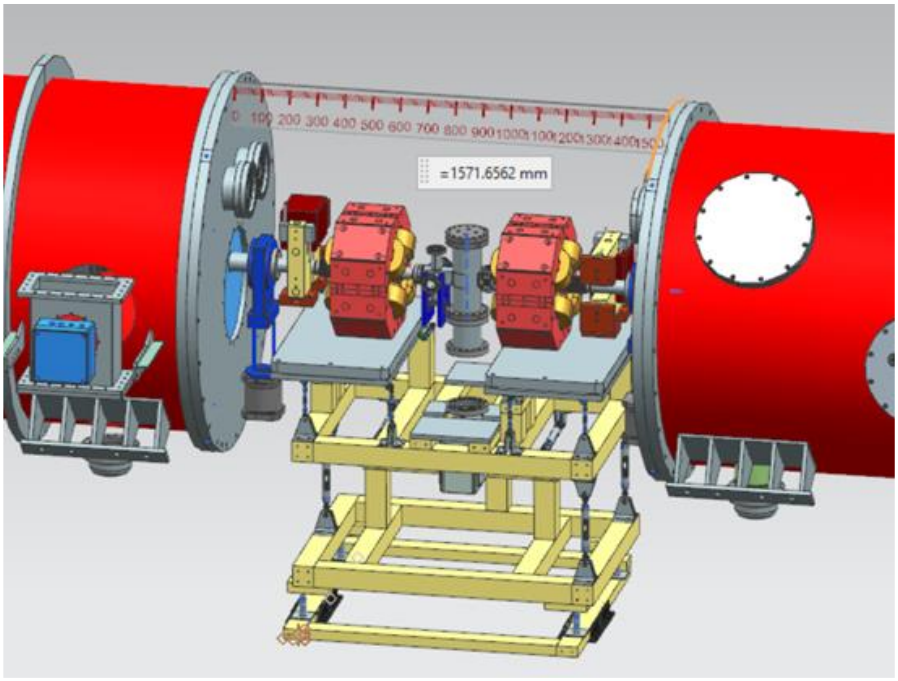

Figure 9: Finished model of HB-650 Warm Unit frame

Previous work on this project has included finalization of the HB-650 Warm Unit frame, as seen in Figure 9 [5]. Analysis was also done previously to determine the modes of the system in the worst-case scenario, which can be seen in Table 1Table 2 [6]. It was also found through simulation that none of the expected modes would fall below the minimum allowable frequency of 15 Hz.

Mode	Frequency (Hz)
1	17.559
2	27.908
3	32. 573
4	36.383
5	69.73
6	83.029

Table 2: Modal Analysis Results [6]

Modeling has also shown that the frames will be able to easily meet expected loading limits indicated in Table 3 in which the results of these analysis show that the material stresses of the frame are orders of magnitude less than their yield requirements.

Label	***Force reading (N)***	***Maximum Allowable Force (N)***
Turn Buckle		
Lower Raft:		
Transverse Right	3.9	23514
Transverse Left	3.9	23615
Beam Direction	1.2	23616
Single Right Vertical	1932.6	23617
Front Left Vertical	965.2	23618
Back Left Vertical	942.1	23619
Left Upper Raft:		
Front Vertical	22.3	25199
Back Outside Vertical	149.7	25200
Back Inside Vertical	299.4	25201
Front Beam Direction	14.1	25202
Back Beam Direction	0.4	25203
Transverse	28.2	25204
Right Upper Raft:		
Front Vertical	65.3	25207
Back Outside Vertical	171.9	25208
Back Inside Vertical	277.1	25209
Front Beam Direction	2.5	25210
Back Beam Direction	16.7	25211
Transverse	1.8	25212
	Stress Reading (MPa)	***Maximum Allowable Stress (MPa)***
8020 Maximum Stress	12.6	241
Bracket Maximum Stress	44.3	240

Table 3: Structural Analysis Nominal Configuration Results Summary [6]

Furthermore in a simulated catastrophic failure it was found at the mass would still be transferred into the three vertical struts as a failsafe mechanism. Additionally worst-case loadings scenarios were examined, are exemplified in Table 4, and the Warm Unit frame was shown to be capable of the various loading conditions.

Label	*Force reading (N)*	*Maximum Allowable Force (N)*
Turn Buckle		
Lower Raft:		
Transverse Right	25.5	23514
Transverse Left	111.1	23615
Beam Direction	64.2	23616
Single Right Vertical	1902.2	23617
Front Left Vertical	907.1	23618
Back Left Vertical	1049.6	23619
Left Upper Raft:		
Front Vertical	12.7	25199
Back Outside Vertical	39.2	25200
Back Inside Vertical	198.8	25201
Front Beam Direction	3.5	25202
Back Beam Direction	9.7	25203
Transverse	7.2	25204
Right Upper Raft:		
Front Vertical	78.6	25207
Back Outside Vertical	159.4	25208
Back Inside Vertical	252.5	25209
Front Beam Direction	0.5	25210
Back Beam Direction	21.9	25211
Transverse	0.01	25212
	Stress Reading (MPa)	***Maximum Allowable Stress (MPa)***
8020 Maximum Stress	14.4	241
Bracket Maximum Stress	43.6	240

Table 4: Worst Case Loading Results Summary [6]

A rudimentary test list for the assembled frame including the following, Translation of struts through full extension and retraction individually and in combination, Confirmation of the position and rotation limits of upper magnet support and the full raft, Ability to maintain three-point contacts with rails, Structural tests that will exceed expected loads by at 50%, Vibration tests with impact hammers to quantify the resonance frequencies of the structure.

1.4 BRIEF OVERVIEW OF PROJECT

This project aims to evaluate a physical stand capable of accommodating 6 degrees of freedom (DOF) adjustment within a range of +/- 30 mm. It is also tasked with integrating a secondary stage, allowing for another 6 DOF adjustment with a range of +/- 15 mm for each magnet corrector package. Crucially, the stand must maintain instrumentation within a 1.3 m do-not-exceed envelope and align it precisely with the proton beamline.

The stand's design must also account for mass production, as it will need to support a total of 13 warm unit sections between the HB-650 cryomodules as seen in Figure 10.

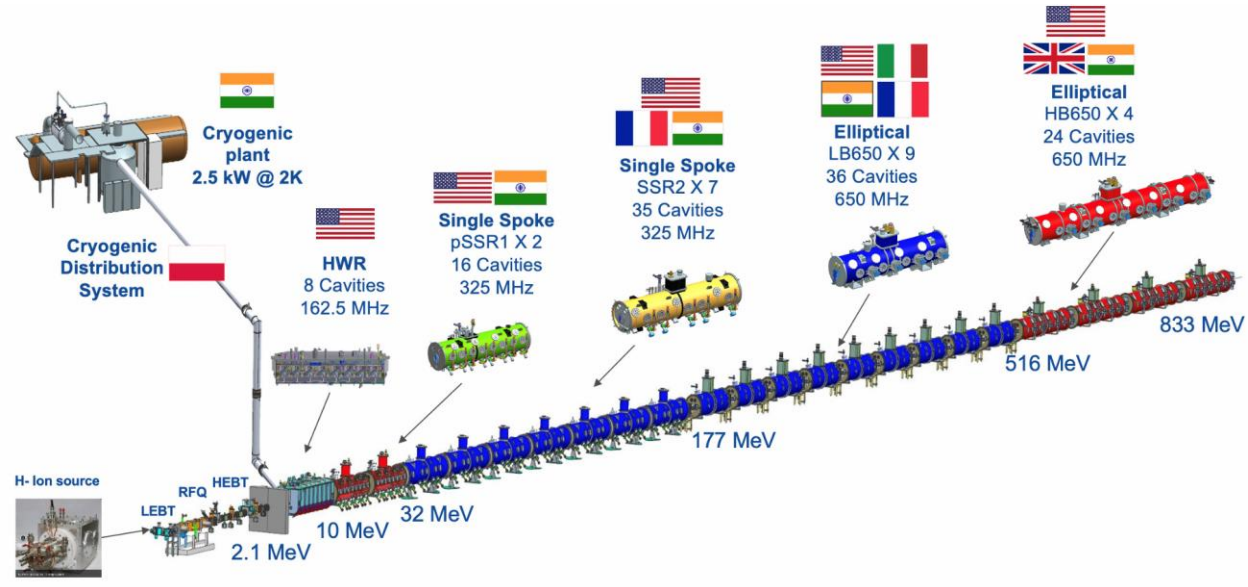

Figure 10: PIP-II upgraded Linac [1]

A primary consideration is ensuring the stand can comfortably support the 1100 kg instrumentation in all adjustment positions, necessitating the identification and analysis of its worst-case position.

Moreover, it is vital to validate the various loading conditions of the stand and highlight key assembly and installation points. Additionally multiple tests will be used to determine and confirm the frequency response even when in the face of various inputs. This will provide

technicians with a comprehensive understanding of what to expect during assembly and installation of these stands.

2. ASSEMBLY

To complete this thesis the successful assembly of the frames as well as testing of the extreme conditions and confirming that the frames stay within specified ranges needs to be shown. Alongside the assembly and testing technicians and engineers at Fermi National Laboratory should be provided instructions of the best practices to assemble these frames.

2.1 OVERVEIEW

A significant outcome of this thesis is the successful completion of test assemblies for both the HB-325 and HB-650 Warm Unit frames. The subsequent sections will delve into the necessary steps to accomplish these assemblies, along with key insights gleaned from these two test assemblies that can inform future assembly and installations, particularly concerning the final installation of all 13 of the frames.

Providing the assembly process for the HB-325 and HB-650 Warm Unit frames was a critical aspect of this thesis, offering practical insights into the nuances of such intricate constructions. By dissecting the steps involved, we can not only understand the intricacies of these specific assemblies but also glean valuable lessons that can be applied to future projects. The assembly process of these frames primarily involved utilizing 8020 beams of various sizes. [7] These beams were then modified to be better able to be connected by Steiner. Furthermore, certain frame parts were fabricated through Fermi National Lab's local machine shop, namely, the turnbuckles and the platforms the equipment would interface with. In the initial test, it was discovered that several large beams were missing, necessitating their procurement.

For both the HB-325 and HB-650 Warm Unit frames, assembly was carried out in stages, progressing from the ground up. Before all the stages were able to be connected together the turnbuckles had to be set to specific thread depth.

2.2 HB-325 WARM UNIT FRAME

Among the two frames, the HB-325 Warm Unit frame is notably simpler, featuring only one set of turnbuckles, thereby resulting in a less complex frame structure as shown fully assembled in Figure 11.

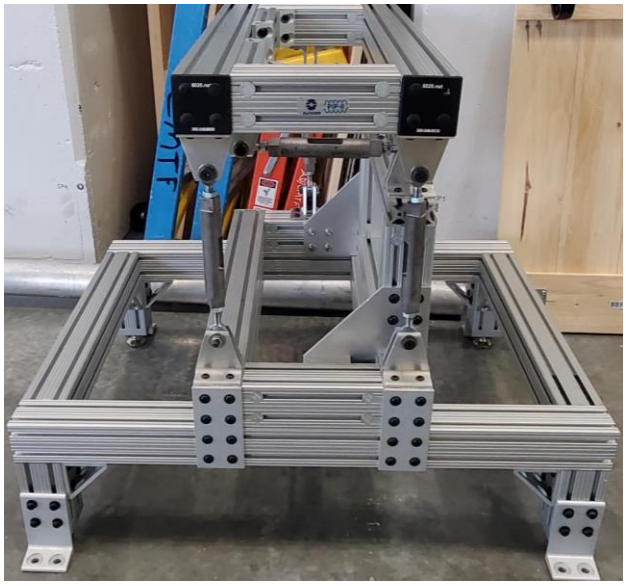

Figure 11: Side view of assembled HB-325 Warm Unit frame

To facilitate ease of assembly and ensure effective quality control checks, the assembly process was divided into four distinct sections: the base layer, mid layer, top layer, and connections between these layers as identified in Figure 12.

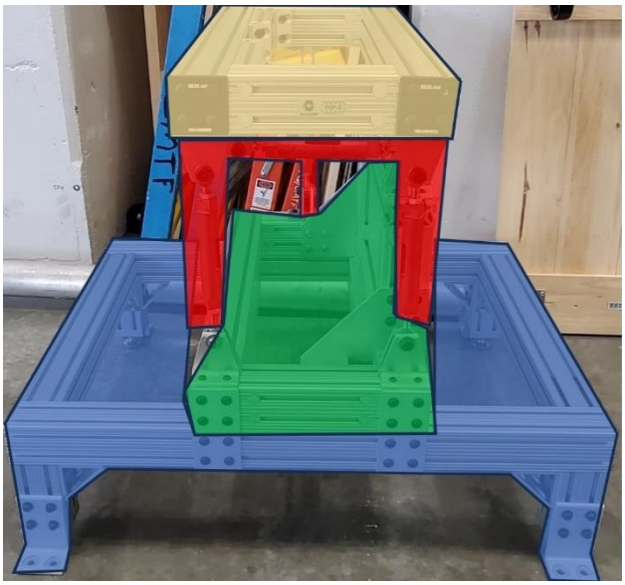

Figure 12: Side view of assembled HB-325 Warm Unit frame with the layers highlighted as follows, base – blue, mid – green, top – yellow, connectors – red

It is important to emphasize that any single layer of the HB-325 Warm Unit frame weighs less than the 50 lbs. limit for a person to carry. However the full assembly of the HB-325 Warm Unit frame weighs more than 50 lbs. and therefore should not be attempted to be moved by an individual without additional equipment.

The provided drawing of the base layer of the HB-325 Warm Unit frame can be seen in Figure 13. The base layer comprises a box frame with two central supporting beams, each supported by four feet as stipulated in the design. These feet are equipped with self-leveling threaded rods, enabling them to adapt to varying floor conditions. During assembly, it became evident that the assembly sequence was crucial, as certain steps could not be executed if other beams were obstructing the way. This thesis will describe some of the largest steps needed to be done to assemble the frames however a more detailed list of assembly instructions are included in the traveler which will be provided to Fermi National Laboratory on the conclusion of work done.

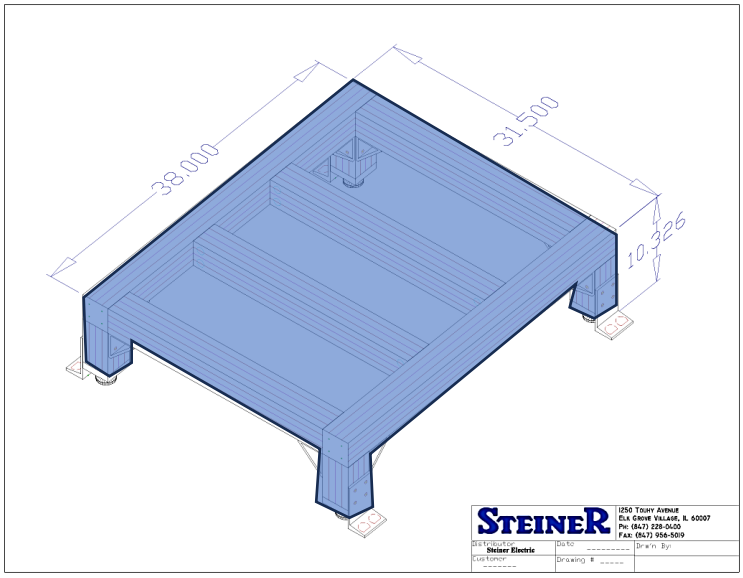

Figure 13: Drawing of the base layer of the HB-325 Warm Unit frame provided by Steiner. Dimensions are in inches.

The subsequent section of the assembly process is the mid part, identified in Fermi Lab's internal system as F10183419 as shown in Figure 14. This section entails the intersection of two boxes at a right angle. It is important to tighten the circled upright supports before installing the topmost beam as after that beam is installed the bolts in the uprights are not able to be accessed to be tightened down. It is also important to mention that this step calls for the inclusion of nuts to be used later in the assembly of the whole HB-325 Warm Unit frame not just the mid layer.

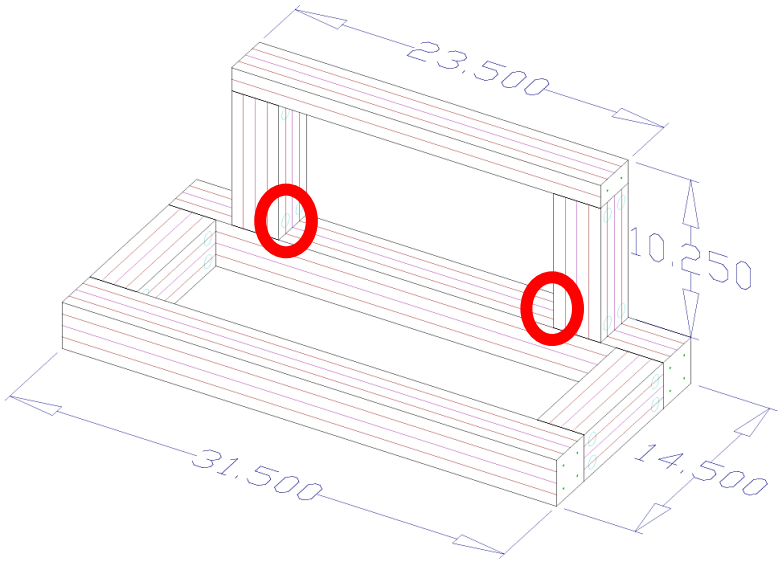

Figure 14: Drawing of the mid layer of the HB-325 Warm Unit frame provided by Steiner. Dimensions are in inches.

Subsequently, the top frame was assembled as shown in Figure 15, designated as F10183421 in Team Center. This frame serves as the platform for an array of characterization sensors. It is a two-dimensional square structure with various supporting pieces. Once again, it is imperative to adhere to the prescribed assembly sequence, as certain nuts and bolts may not be able to be installed without disassembly of the entire layer if assembled in the wrong order.

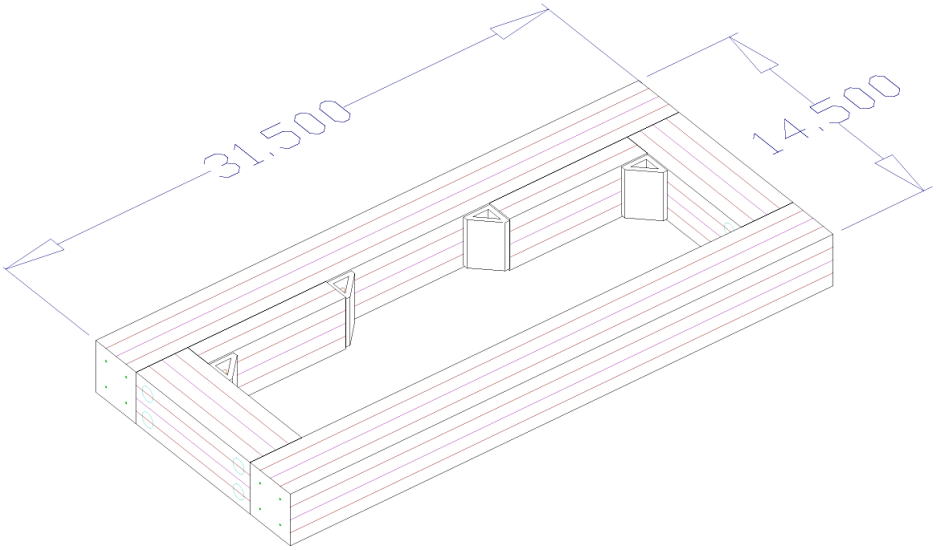

Figure 15: Drawing of the top layer of the HB-325 Warm Unit frame provided by Steiner. Dimensions are in inches.

The final step of the HB-325 Warm Unit frame assembly process involves integrating the three previously discussed parts to prepare it for use. This is accomplished by connecting the middle part to the base utilizing an aluminum plate and preset nuts. Then attach the turnbuckles, shown in Figure 16, to the middle layer, and finally link the turnbuckles to the top layer.

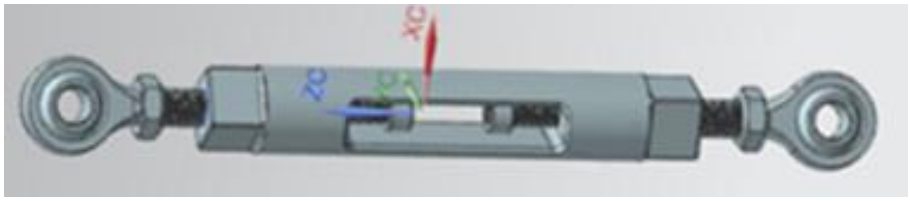

Figure 16: Turnbuckle

Before all nuts are tightened, a plum line is used to verify that the top plate is vertically aligned. Subsequently, a level is employed to ensure that the assembly is level. Although the turnbuckles allow for a wide range of motion to overcome unevenness at this stage of the assembly process, it is recommended to set up the system as accurately as possible. This is to ensure that the maximum modification can be saved in case those adjustments are needed at the final installation site.

Future plans for the turnbuckles include the creation of some sort of mechanism that sets the initial rod end separation as well as the original distance from the center. This with set the treads of the rod ends to be 50% engaged in nominal conditions in order to maximize available travel length.

2.3 HB-650 WARM UNIT FRAME

As previously mentioned, the HB-650 Warm Unit frame assembly is the more intricate of the two assemblies shown fully assembled in Figure 17.

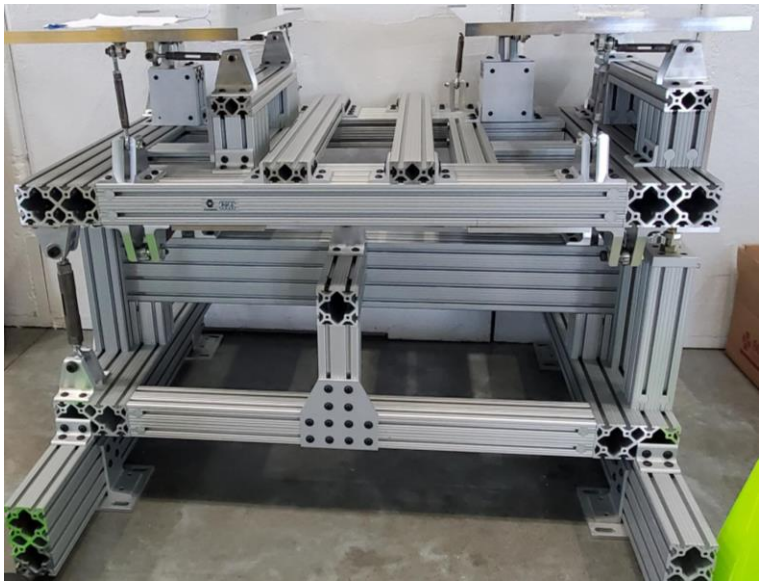

Figure 17: Front view of assembled HB-650 Warm Unit frame

This outline will describe the assembly process starting from the base layer, then to the mid layer then the top layer Figure 19-21. As shown in Figure 18 there are two layers of turnbuckles one from the mid layer to the top layer, circled in red, and a set of smaller turnbuckles from the top layer to the corrector magnet plates circled in circled in yellow.

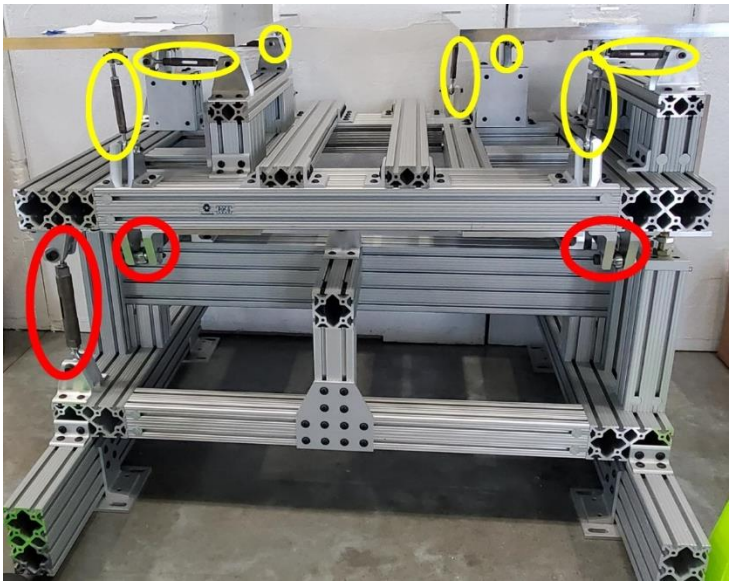

Figure 18: Front view of assembled HB-650 Warm Unit frame with large turnbuckles circled in red and small turnbuckles circled in yellow

Minimal assembly is required for the two feet as shown in Figure 19, as they are essentially beams housed within a C-channel, which enables them to be secured to the floor. However, it is necessary to preset some nuts ahead of time, as specified in the traveler. It is worth noting that the brackets affixed to the top side of the beams should be kept loose, facilitating the manipulation of the middle section into place.

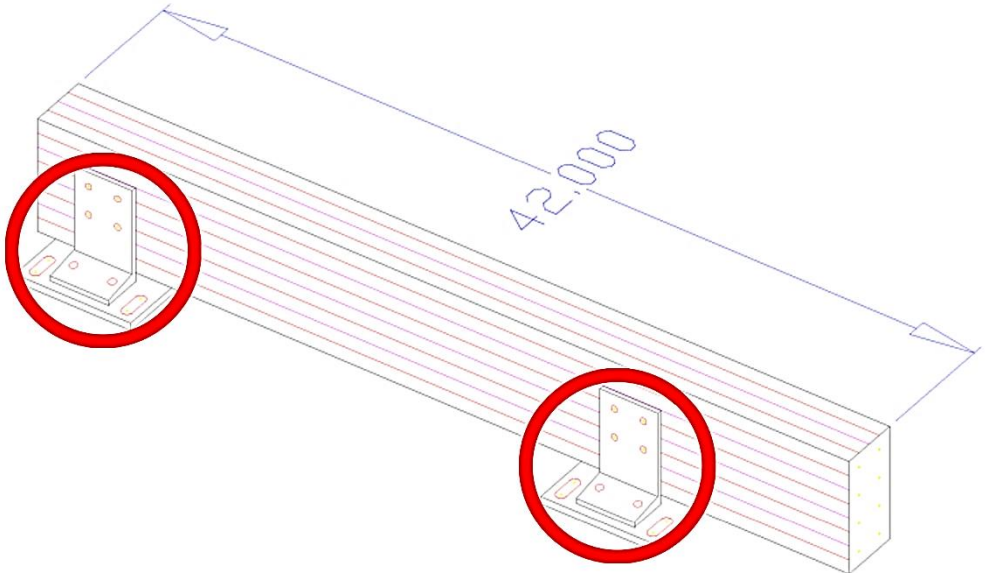

Figure 19: Drawing of the base layer of the HB-650 Warm Unit frame provided by Steiner. Dimensions are in inches.

The middle section, as shown by Figure 20, of the assembly is notably intricate, and it is strongly advised to strictly adhere to the instructions outlined in the traveler. A few deviations from the original design were implemented, as it was determined that the diagonal brace support was unnecessary, and this part was not provided based on recommendations from Steiner. Moreover, numerous metal plates serve not only as structural support but also contribute to the overall damping of the system.

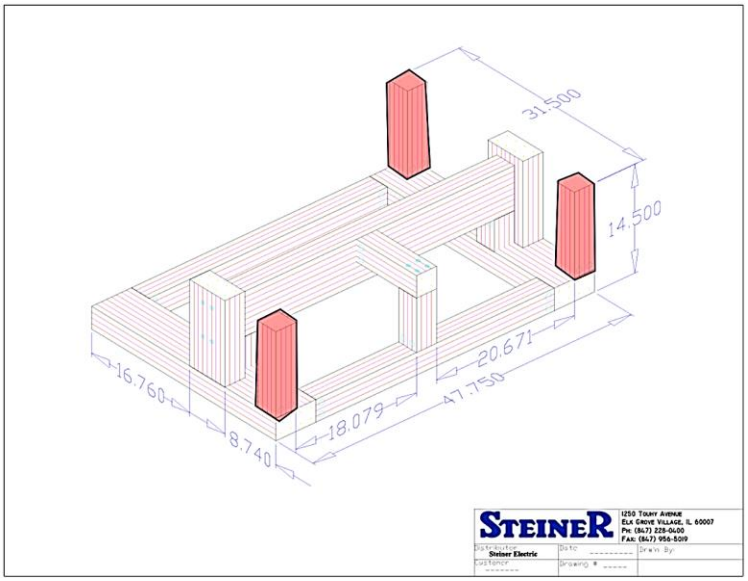

Figure 20: Drawing of the mid layer of the HB-650 Warm Unit frame provided by Steiner. Dimensions are in inches.

It is crucial to highlight that the middle section features three vertical posts, highlighted in red in Figure 20, designed to mitigate the risk of the top part falling. These posts can also be adjusted to both dampen the movement of the top part along with being designed to prevent the top layer from crashing down.

In the assembly of the top part, it is crucial to adhere to the instructions meticulously. Failure to do so may result in the back plate being exceedingly difficult to attach, and some beams may not be securely held in place.

A noteworthy aspect of the top part of the HB-650 Warm Unit frame, as shown in Figure 21, is that it needs to be flipped multiple times during assembly. Additionally, it is advisable to assemble it partially on its side. This is due to the fact that the base plate used for vibration damping must be inserted into the back before brackets for the turnbuckles are applied. Once this is done, the top part can be flipped back over to apply the turnbuckles, thus completing the assembly of the top part.

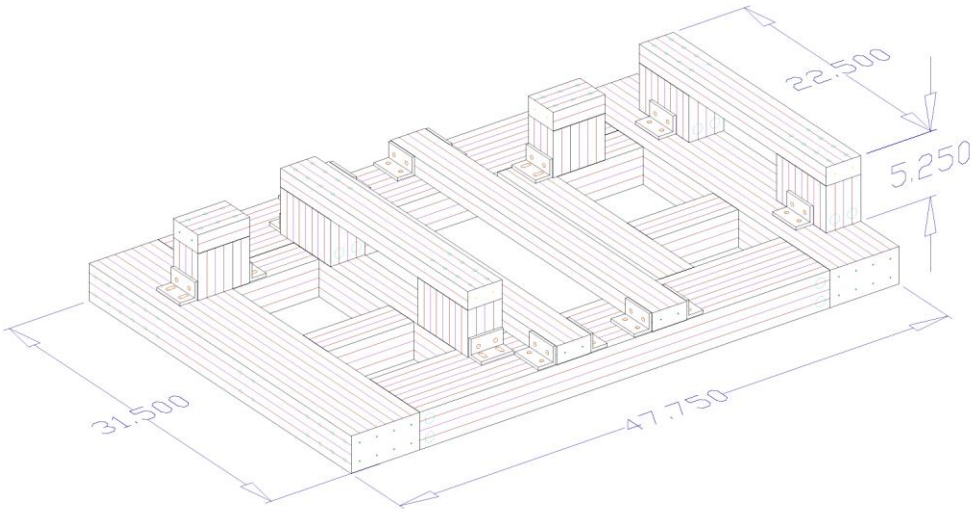

Figure 21: Drawing of the top layer of the HB-650 Warm Unit frame provided by Steiner. Dimensions are in inches.

It is imperative to consider utilizing a mechanism to support the HB-650 Warm Unit frame during most of the assembly process, as it will often be elevated in the air. This precaution is essential to minimize the risk of potential damage or injury to the individual assembling it. This is particularly critical when connecting the different stages, as they will not be entirely secured by the turnbuckles and will often be positioned above the head of the technician assembling the frame.

Upon completion, the HB-650 Warm Unit frame will be characterized by the presence of two base plates, serving as platforms for the quadrupole magnets. It is noteworthy that during the assembly of the HB-650 Warm Unit frame in this test, one of its legs needed to be procured after the initial order.

A key thing to note regarding the assembly of the HB-650 Warm Unit frame is that the C channel, circled in Figure 19, will be preinstalled in the final location. A brass plate will be installed as well to allow the entire HB-650 Warm Unit frame assembly to slide into place.

2.4 DIMENSIONAL CHECKS

A comprehensive range of measurements was undertaken to guarantee the precise sizing of the stands. Primarily conducted prior to the completion of assembly, this process ensured the presence of all listed materials, allowing for the identification of any missing components and the subsequent procurement thereof.

Utilizing a tape measure, a technician assembling the frame was encouraged to mark the measured piece to indicate its size. Beyond the use of a tape measure, the inclusion of a level and calipers, particularly for bolts and brackets, was recommended. While the majority of measurements were executed pre-assembly, post-assembly measurements were also conducted to ensure the correct positioning of the frames, a pivotal aspect, particularly in the HB-650 Warm Unit frame, where the middle and base are adjustable to set the position for the corrector magnets. During this process it was found that the brass plates were a $1/8^{th}$ of an inch too wide which was noted. Fermi National Laboratory have since started to machine down the plates to the new desired sizes.

After initial assembly the warm unit frames needed to be moved due to space constraints. This provided the opportunity to test the background vibrations which will be discussed further in the vibration testing. Due to the move additional measurements were taken at the new location, as seen in Figure 22, to prove that the completed frames could survive transportation with minimal sliding of the parts.

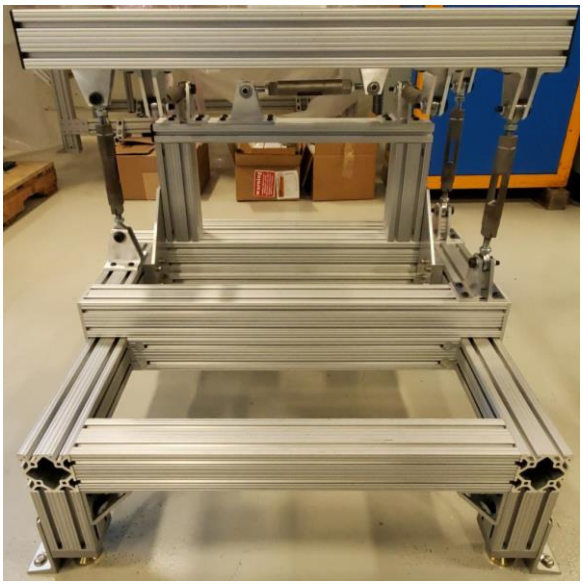
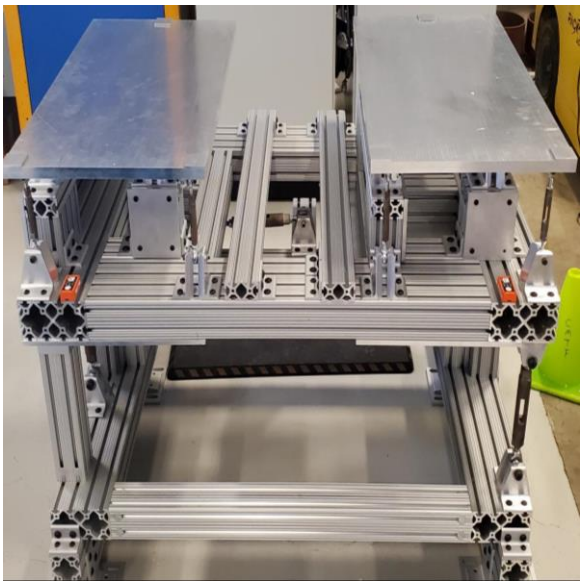

Figure 22: Assembled HB-325 Warm Unit frame at A0 (left) and assembled HB-650 Warm Unit frame at A0 (right)

Both at the initial location and at A0 the Warm Unit frames were within the specified dimensions proving that the design was able to be translated into the real world, the reconfirmation of the dimensions at A0 also proved that the frames could survive transportation. This means that the frames could be assembled offsite if that is found to be more efficient in the future.

2.5 DOCUMENTATION

In order to facilitate the efficient assembly and installation of the Warm Unit frames at Fermi National Laboratory, a comprehensive set of assembly instructions, referred to as the traveler, has been developed. The traveler is meant to serve as a detailed guide for technicians and operators involved in the assembly process.

The development of the traveler involved a systematic approach to provide step-by-step instructions for assembling each part of the Warm Unit frames. The process began with a thorough analysis of the assembly sequence, starting from individual components and

progressing to sub-assemblies and final installations. This layered approach ensures clarity and precision in the assembly process.

The traveler comprises detailed instructions presented in a sequential manner, going layer by layer to guide operators through each step of the assembly process. Each step is accompanied by numbered callouts, as depicted in Figure 23, strategically placed to enhance comprehension and provide visual cues for operators. These callouts are designed to offer a clear understanding of the assembly and installation procedures, hoping to thereby minimize errors, and streamlining the overall process.

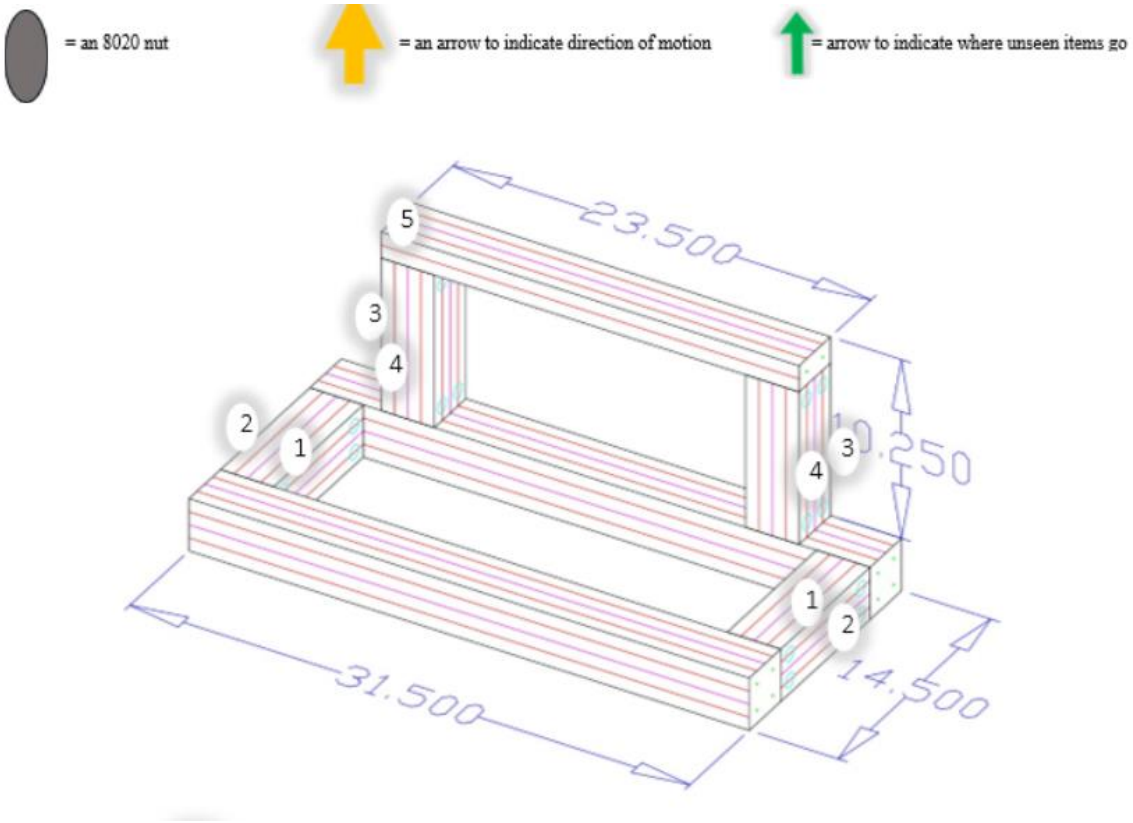

Figure 23: HB-325 Warm Unit frame with numbers indicating the order of assembly

Furthermore, the traveler incorporates insights and lessons learned from previous assembly experiences, ensuring best practices are integrated into the instructions. Feedback from technicians and operators during prototype assembly phases was also considered to refine the

traveler and optimize its usability. By providing a comprehensive and user-friendly assembly guide, the traveler aims to enhance efficiency, accuracy, and safety during the assembly and installation of the Warm Unit frames at Fermi National Laboratory.

One of the primary focuses of the traveler is to highlight specific critical steps and considerations that are vital for successful assembly. For instance, a notable point highlighted in the traveler is the necessity to flip over the top layer of the HB-650 Warm Unit frame multiple times during assembly. This step is emphasized due to its critical nature in achieving successful assembly and alignment.

Furthermore, the traveler places significant emphasis on the order of operations during assembly. Adhering to the prescribed sequence is crucial to avoid potential setbacks such as having to disassemble and reassemble a layer or, in extreme cases, the entire frame. This emphasizes the importance of following the prescribed sequence meticulously to prevent unnecessary rework and ensure efficiency.

Another key aspect addressed in the traveler is the precise spacing and initial depth settings for the turnbuckles. This detail is crucial to facilitate smooth installation and alignment of the turnbuckles across different layers of the frame and will hopefully turnbuckle assemblies as seen in Figure 24. When turnbuckles are not set properly the total rotation space of the traveler is limited. The traveler provides explicit instructions on the required spacing and depth settings to optimize the installation process.

Figure 24: Turnbuckle with an uneven initial rod depth set

Additionally, the traveler outlines the specific hardware and additional components needed to attach the turnbuckles effectively. This includes identifying the varying requirements for different sections of the frame and the potential need for extra spacers to eliminate any slack and ensure proper alignment. A selection is provided in Figure 25 of some of the ball rod end mounting setups.

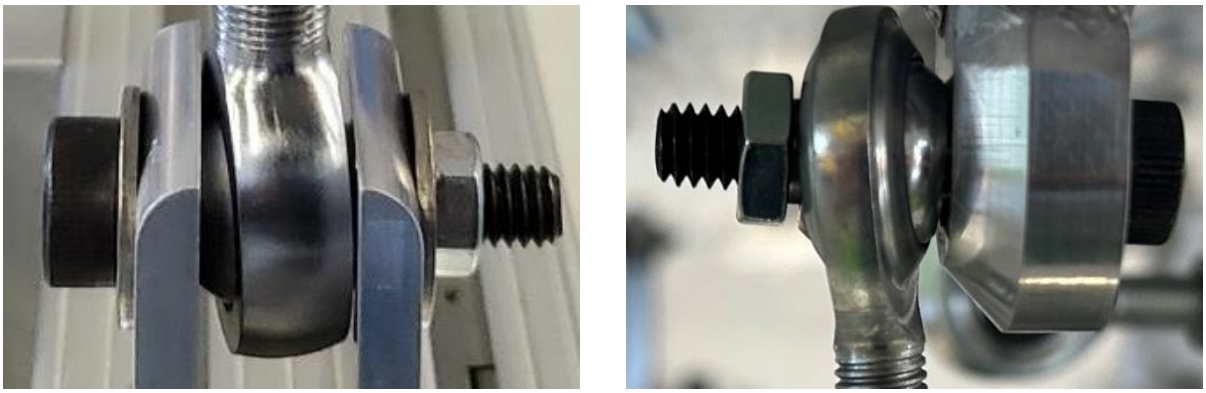

Figure 25: Different ball rod end mounting setups with a double bracket mount (left) and a plate mount (right)

By incorporating these detailed instructions and highlighting critical steps and considerations, the traveler serves as a comprehensive guide to support technicians in executing the assembly process accurately and efficiently, ultimately contributing to the successful completion of the Warm Unit frame assembly.

2.6 ASSEMBLY CODE COMPLIANCE

The WURM stand must meet the functional requirements as well as the safety requirements of FESHM [9]. There are many FESHM chapters and codes that guide the design, but the main chapter that drives the WURM stand is FESHM Chapter 5100: Structural Safety [8]. Chapter 5100 dictates that the design be comprised of common materials and fasteners, have clear load paths, have relatively low failure modes, and be further governed by appropriate US safety codes [9]. The chapter also compiles any code that a structure may be governed by. The

codes that pertain to the WURM stand are ASCE 7: Minimum Design Loads for Buildings and Other Structures, ADM1: Aluminum Design Manual, and AWS D1.1: Structural Welding Code – Steel. ASCE 7 dictates that the allowable stress be 60 percent of the yield strength. If the experienced stress is lower than the allowable stress, then the structure is deemed acceptable [8]. ADM1 dictates that the allowable stress is defined by the yield stress divided by a predetermined factor of safety for aluminum structures [11]. All analyses performed thus far meet the specifications set by FESHM Chapter 5100 as shown in Table 5: Materials-Based Allowable Stress.

Material	Yield Strength (MPa)	Allowable Stress (MPa)	Highest Stress (MPa)
4140 Steel	417	250.2	240
Mild Steel	200	120	50
6105 T5 Aluminum (8020)	140	84	7.1
3103 Aluminum	175	105	17.1
Alloy Steel (Bolts)	249	149.4	65.6

Table 5: Materials-Based Allowable Stress

Other safety concerns that are stated by FESHM Chapter 5100 are the additions of international building codes to the parameters which is explained further in ASCE 7. ASCE 7 contains many safety guidelines as they pertain to buildings such as seismic loading, wind loads, and loadings due to snow, which do not pertain to the WURM stand design.

2.7 FUTURE ASSEMBLY UPDATES

Multiple fixes to the turnbuckles were identified and included in assembly and procurement instructions. The two main suggestions were to modify the ball rod ends to make the tolerance of the race precise. A temporary fix was identified where a technician would apply to the ball ends a slight layer of Loctite to achieve a similar result. Additionally a shadow box is being designed to ease the turnbuckle assembly process with the thread depth set for the technician.

The plate highlighted in Figure 26 was identified as not being needed as the HB-650 Warm Unit frame was able to damp vibrations to the necessary levels without the plate. Because of this the plate was removed from the assembly instructions and orders. The removal of this plate from the assembly steps allows for a decrease in cost and difficulty of assembly.

Figure 26: HB-650 Warm Unit frame with stiffening plate to be removed highlighted

Finally the last change from the previous work was a requiring a tighter tolerance of the turnbuckle mounting brackets as seen in Figure 27. During the test assembly it was found that the current size of the through hole was too large and therefore allowed for a large amount of play in interface between the shoulder bolt and the bracket.

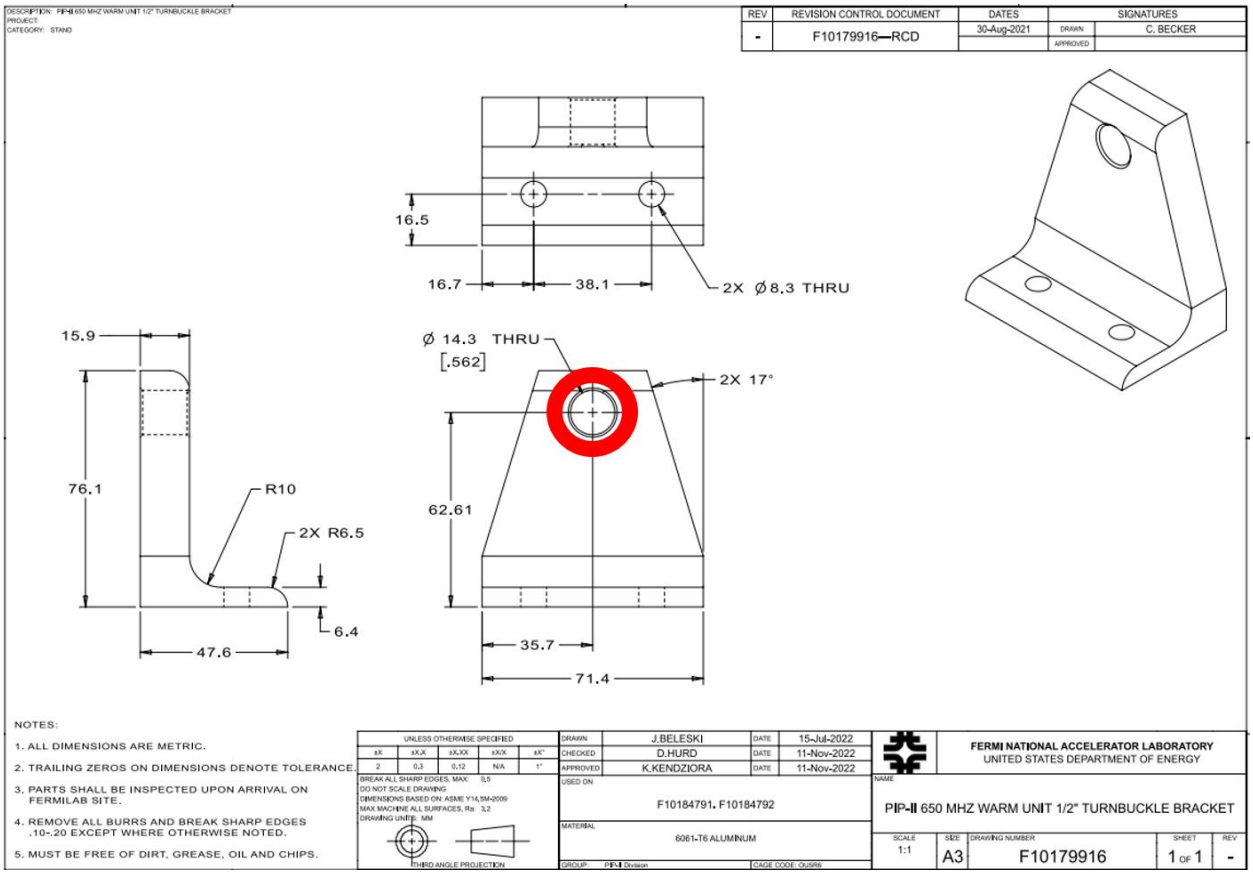

Figure 27: Drawing of the 1/2" turnbuckle bracket

It should also be noted that the time to fully assemble and install all the frames was extrapolated from the time it took to assemble and install the two test frames. The estimated time to complete all of the assemblies was found to be at six to eight hours per assembly for a total of thirteen days of working after a technician has grown used to how to assemble which means an allowing for a learning curve an estimation of twenty days in total to assemble all of the frames needed and additional three days is estimated for the installation and testing processes as well as another two days for confirmation of magnet installation to the frames. In total it is estimated that to fully assemble and install the frames about a month of a technician dedicated to these frames is needed.

3. VIBRATION TESTING

Vibration testing plays a crucial role in verifying that the frames conform to the necessary natural frequency ranges. This section provides an overview of the methodology employed in conducting vibration tests to assess the dynamic behavior of the frames.

The testing protocol commenced with impact tests to ascertain the natural frequency of the frames and to gauge the inherent level of dampening within the system. These initial tests provided valuable insights into the structural response and damping characteristics of the frames under moderate impacts.

Following the impact tests, a low-energy oscillating input was applied to analyze low amplitude vibrational transfer within the system and assess the decay of vibrations throughout the structure. This phase of testing aimed to evaluate the system's response to low-frequency oscillations and its ability to dissipate vibrational energy over time.

Subsequently, a more rigorous oscillating input was introduced to simulate a worst-case scenario and assess the impact on the magnet. This phase of testing was particularly crucial in understanding the resilience of the frames under intense vibrational loads, providing insights into their ability to withstand challenging operational conditions.

By employing a systematic approach to vibration testing, including impact tests, low-energy oscillation analysis, and vigorous oscillating inputs, a comprehensive understanding of the frames' dynamic behavior and response to varying vibrational inputs was achieved. These tests were instrumental in validating the frames' design integrity and their suitability for operational deployment. To do that the Warm Unit frames needed to be out of the frequency range of 0-15 Hz. as well as avoiding multiples of 60 Hz. This requirement is due to the want to avoid induced oscillations of the work environment which has been found to have background frequencies to be below 15 Hz. and frequencies from the electric grid of 60 Hz. To determine

the damping coefficient or the factor of time that it takes for and impacts vibrations to decrease magnitude sensors were utilized to record the vibration of the frame.

3.1 OVERVEIW

While raw data was utilized primarily for damping characterization, a significant portion of the analysis focused on the frequency domain. The fast Fourier transform (FFT) emerged as the preferred method for frequency domain analysis due to its rapid processing speed and precision. Upon conversion to the frequency domain through FFT, the identification of natural frequencies becomes feasible, as long as the resonance frequency is within half of the operating frequency. This requirement stems from inherent properties of FFTs and serves as a reliable indicator of the system's resonance behavior. [12] The presence of peaks associated with either input or resonance frequencies indicate the high amplitudes present in the frequency domain, as seen in Figure 28, where the fans resonance frequency can be seen by the repeating peaks at multiples of 29 Hz.

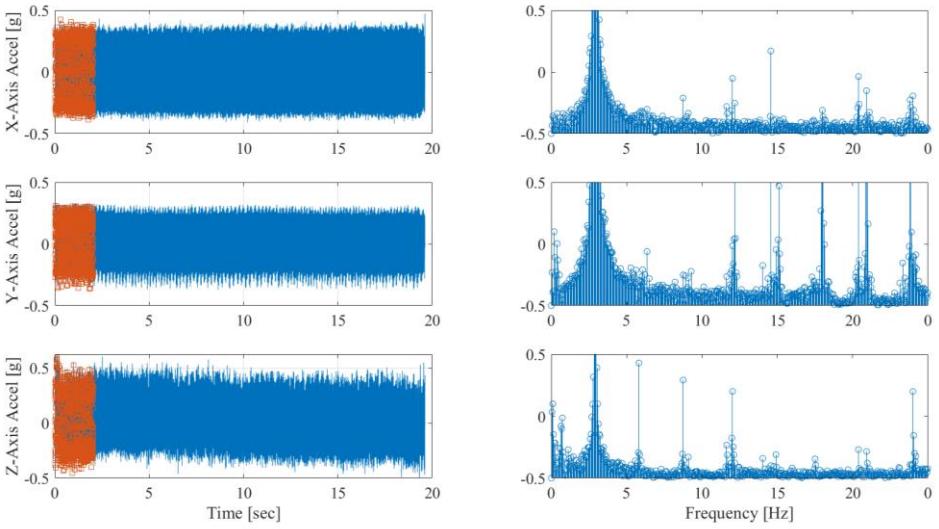

Figure 28: Graph showing the frequency domain of an object who has a resonance at 29 Hz.

Multiple trials were conducted for each test at multiple locations and directions to allow for the isolation of confounding variables. An average response for a given energy input type, sensor location, input location or input direction could be found through careful sorting and labeling of the data. This approach ensured a more accurate assessment of the frames' dynamic behavior and their ability to dampen vibrations effectively [12-15]. As well as the ability to isolate different variables to be more efficient in the number of tests needed.

Different locations and directions were deliberately chosen for energy input during tests to understand how energy injection into the system influenced damping capabilities across the frames. This systematic variation in energy inputs provided valuable insights into the frames' performance under varied operational conditions, aiding in the identification of optimal damping strategies.

3.2 SENSORS UTILIZED

EnDAQ S4 Vibrational Sensors, as shown in Figure 29, were used in order to determine the vibrational frequencies of the frames.

Figure 29: An image of an enDAQ S4 Vibration Sensor [16]

The vibrational sensors were attached to the frame through the use of double-sided tape with an attempt being made to keep all sensors aligned in the same coordinate system. Each sensor records data in the x, y, z and time axis. these coordinates are then aligned with the three axis of the beam, beamline, gravitational and, perpendicular. In the cases where it was not possible to align the sensors in the same way the sensors were rotated orthogonally with each rotation being recorded. this record was then used to rotate the data such that all of the data was aligned and ordered the same. The data collection rate for these sensors was set to be 500 Hz. This rate was selected because it gave the highest level of resolution allowing for the most accurate results [16]. This rate also allows for the ability to see a range of frequencies that fully covers the critical worrisome low frequencies identified as well as including the first couple of multiples of 60Hz.

In order to retrieve the data on the sensors the EnDAQ provided program was used. An additional benefit of this program was that it allowed for an initial display for the time required to fully damp the system. the rough estimate was found to be ~1 second. This was later confirmed through MATLAB and found to be closer to .1 second as seen in Figure 30. Identifying the time needed to achieve near initial state allowed a shorter time between tests to increase the number of tests that were able to be recorded.

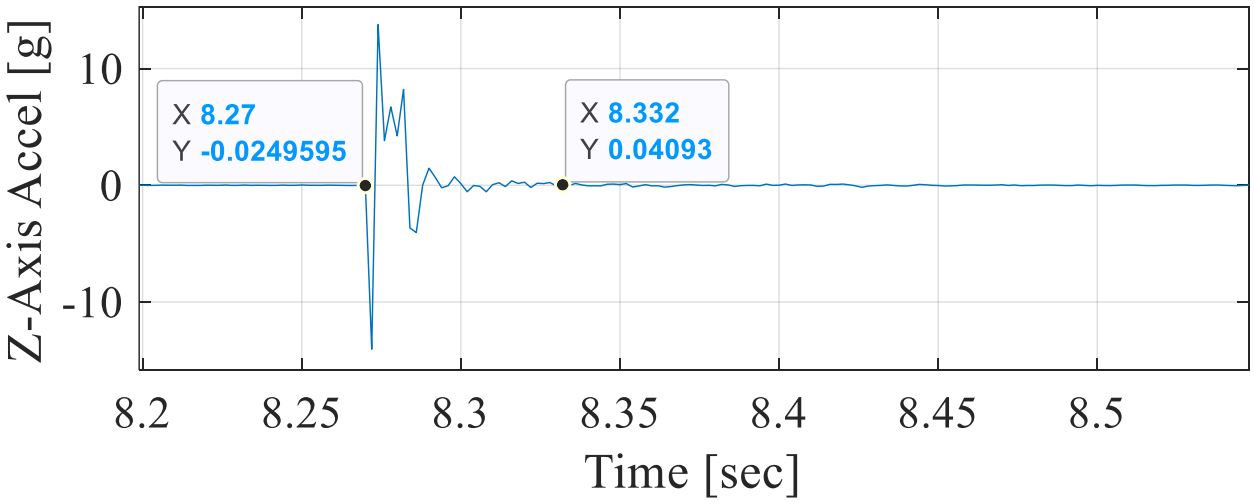

Figure 30: An acceleration (g) over time (s) graph showing the time needed for the energy to decay to original levels

3.3 PROGRAMS USED

Following the conversion of data into a CSV file format, the analysis process involved the utilization of MATLAB scripts designed specifically for reading and analyzing the acquired data. The development of these scripts involved a collaborative effort, with a significant portion of the code utilized for parsing data being contributed by Fermilab employees, namely Adam Wixson and Jeremiah Holzbauer. Their expertise and contributions were instrumental in developing efficient code for data manipulation and extraction.

Furthermore, specific data analysis tasks necessitated the creation of additional MATLAB scripts tailored for the objectives of this thesis. These scripts were designed to perform customized analyses and extract insights relevant to the specific requirements of the research.

The MATLAB scripts employed a variety of functions and algorithms to process the data, including parsing, filtering, and statistical analysis. The scripts were structured to handle large datasets efficiently while ensuring accuracy and reliability in the analysis results.

3.3.1 PARSING

The first MATLAB script, referred to as "parse," was primarily developed to parse the data obtained from .csv files and convert it into .mat files, enabling seamless integration for further analysis. One of the key functionalities of this script was to filter and retain data sampled at the 500 Hz. sampling frequency, a decision made to optimize processing power and align with the specific requirements discussed earlier. Additionally, the "parse" program was responsible for aligning the data from different sensors in time, ensuring synchronization for accurate analysis.

The "parse" program was designed to locate raw data files within designated folders, identified by specific leading identifiers such as "SS" followed by sensor-specific numbers, as per the labeling conventions from the enDAQ software utilized with the sensors. The script targeted four specific channels (channels 08, 32, 80, and 43), where acceleration and time data were retrieved. That data was then synchronized in time with the appropriate modifiers derived from the sensors' onboard clock.

Upon completion of parsing and alignment, the data was saved in a new format with additional tags as .mat files, ready for subsequent analysis and processing. This process was repeated iteratively for each set of raw data transferred from the sensors' tests, with each test generating a set of three data files corresponding to each sensor utilized. In cases involving more than three sensors, the script accounted for additional data sets for each new sensor, ensuring comprehensive data handling across all sensor inputs.

The robust functionalities embedded within the "parse" script exemplify a systematic approach to data processing, alignment, and storage, laying a solid foundation for subsequent analysis tasks within the research framework. Collaboration with domain experts and adherence

to data labeling standards were integral to the successful execution of these data processing procedures.

3.3.2 ANALYZING

Upon completion of time alignment and conversion to .mat format, the data underwent further processing through a dedicated program, henceforth referred to as "analysis," designed to perform in-depth analysis tasks. This section provides an elaborate overview of the methodologies and functionalities integrated into the "analysis" program for comprehensive data analysis.

The "analysis" program commenced by retrieving the location and orientation data of the sensors, previously set in the "parse" program. This information was crucial for determining any necessary adjustments and ensuring accurate data processing. Following this, the program traversed through the files, mirroring the process in the "parse" program, to locate and extract the required data. A temporary file was then generated to store any figures or intermediate results produced during the analysis.

Subsequently, the program initiated a series of steps to prepare the data for analysis. This included setting the desired evaluation time length and executing a for loop to process each sensor's data individually. The initial analysis focused on detecting values above a predefined sensitivity threshold, a criterion derived from prior research [16]. Data exceeding the sensitivity threshold, 1.1g for impacts and, the start of the test for oscillation tests, triggered the subsequent stages of analysis.

One of the primary analyses conducted by the program involved determining the length of data from each sensor trial and establishing corresponding indices. This facilitated the plotting of raw acceleration data, showcasing perpendicular, beamline, and gravitational accelerations in

a structured format as shown by Figure 31. Additionally, an index was created to identify acceleration peaks attributed to impact and vibrational testing, enabling focused analysis around these critical events.

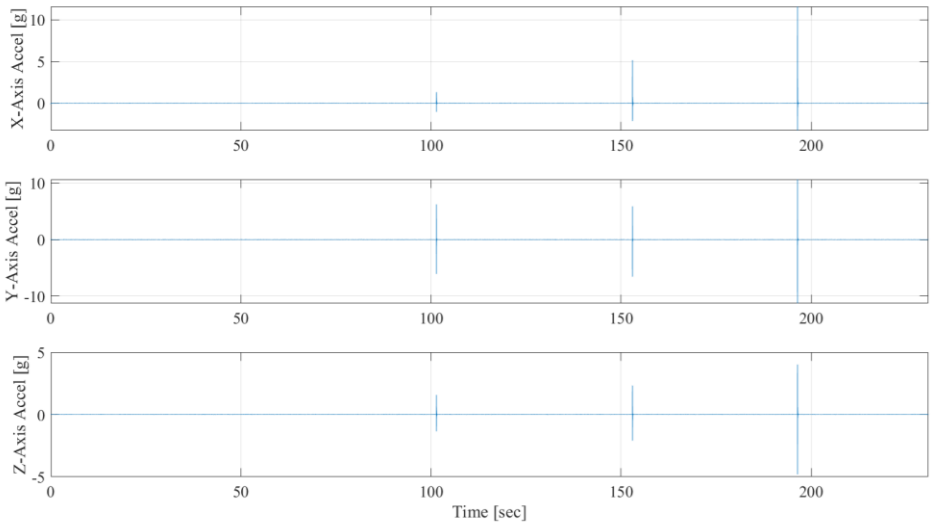

Figure 31: Plot of the acceleration (g) over time (s) without analysis

Markers were strategically placed on the raw data to visualize the time span covered by the analysis with N = 2^ 8 data points for the impact tests and N = 2^11 for the oscillation tests, enhancing clarity and interpretation as seen in Figure 32.

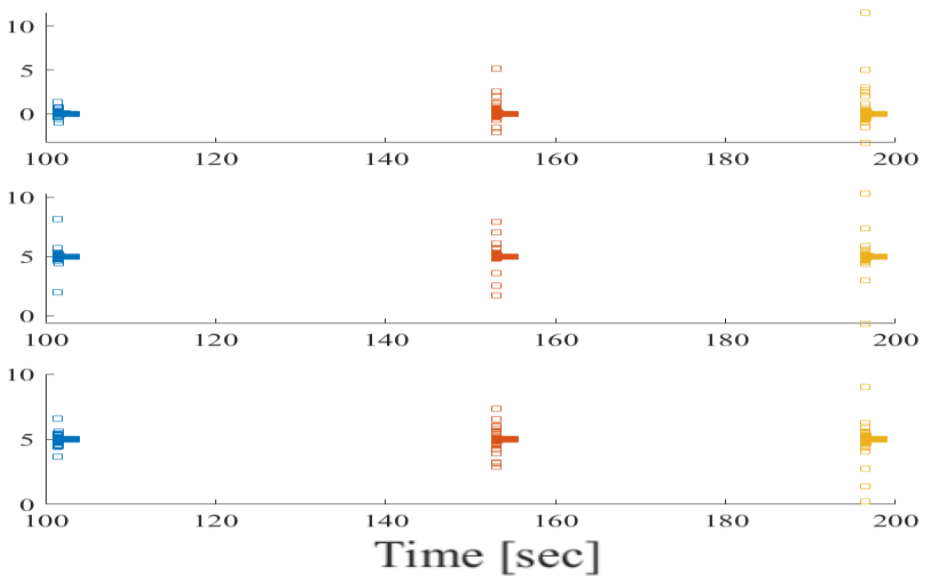

Figure 32: Plot of just the markers to aid in visualization

Subsequently, a stem plot was generated based on the new index to depict the frequency domain. The frequency domain values were determined through utilization of MATLAB's native FFT solver. The data had display settings standardized for consistency and ease of interpretation as highlighted in Figure 33.

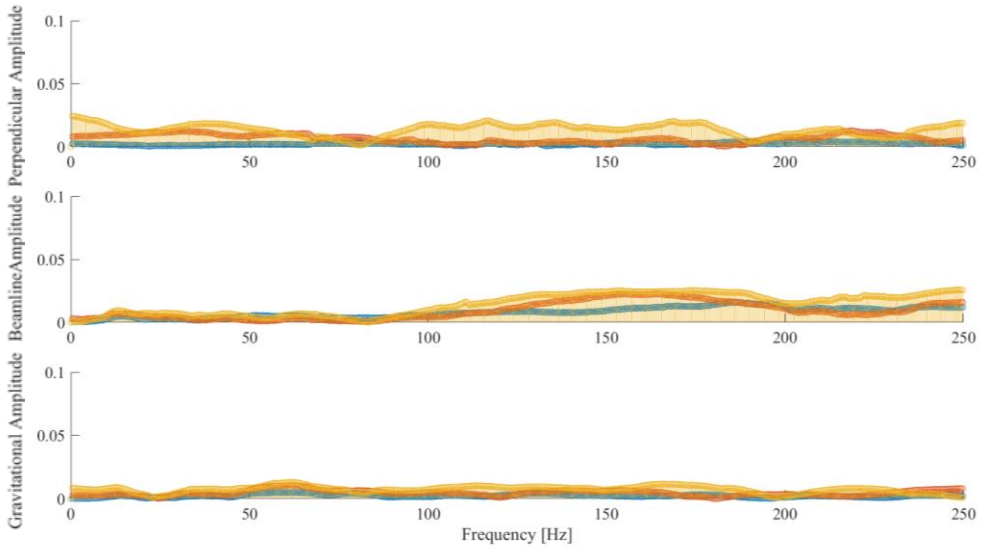

Figure 33: Plot of the frequency domain with the colors of the stem plots corresponding to the color of the markers in Figure 32

Following data visualization, frequency and magnitude information was stored for averaging across multiple files. Averaging and standard deviation calculations were then performed, culminating in the generation of graphical representations displaying these statistical metrics for further analysis and interpretation, as shown in Figure 34.

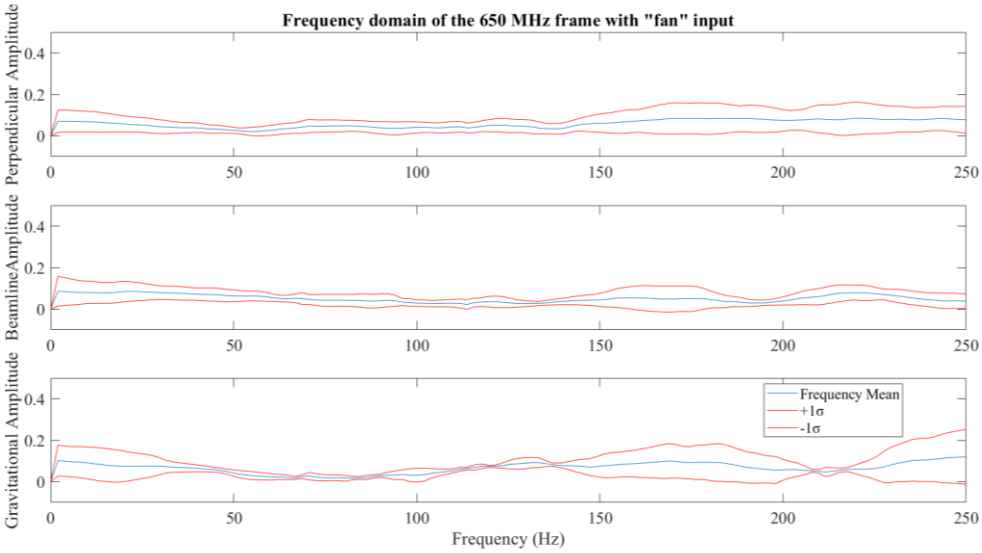

Figure 34: Example of averaged frequency domain

The robust functionalities embedded within the "analysis" program underscore its critical role in extracting meaningful insights from the collected data, facilitating comprehensive analysis and decision-making within the research context.

The code used in this analysis phase exemplifies a combination of existing tools and customized scripts, showcasing a comprehensive approach to data analysis tailored to the unique needs of the research project. Collaboration with experts from Fermilab and the development of specialized scripts contributed to the successful execution of the data analysis process.

3.4 BACKGROUND INPUTS AT A0

After successfully relocating the frames to A0, a series of tests were conducted to assess the background vibrations surrounding the frames. The primary objectives of these tests were

twofold: firstly, to document any significant background vibrations that could necessitate stiffening the frames to enhance the damping coefficient, and secondly, to mitigate the influence of background vibrations on subsequent impact and oscillation tests.

To execute these tests, three enDAQ sensors were activated and left running for a duration of approximately 3 minutes. The collected data underwent thorough analysis using the previously outlined processes. The resultant graph depicting the background vibrations is illustrated in Figure 35.

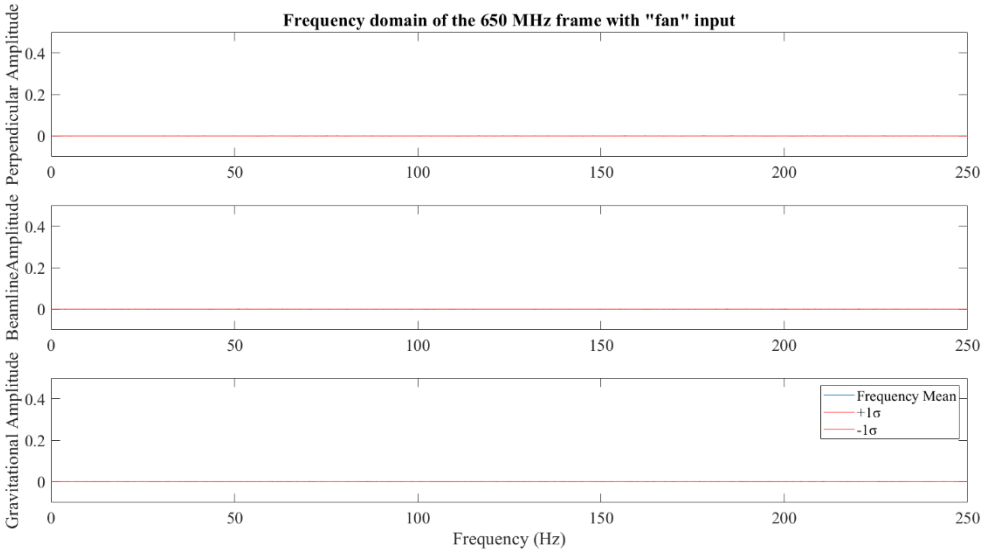

Figure 35: Averaged frequency domain plot of the background vibration on the fully loaded HB-650 Warm Unit frame

The analysis of the collected data yielded promising results, revealing no pronounced low-frequency vibrations affecting the warm unit frames due to background frequencies. While this observation did not directly ascertain a strong damping coefficient, it did instill confidence in this assumption. However, it's essential to note that the absence of detected background frequencies at A0 could also be attributed to the lack of strong background vibrations in that specific environment.

Further investigations were deemed necessary to discern the root cause behind the absence of background frequencies detected by the sensors. These subsequent tests included an impact test aimed at determining the natural frequency of the frame, which could also provide additional validation of negligible background frequency transfer in-between strikes, when the effect of the impact died off. Additionally, an oscillating input applied could confirm vibrational transfer, showcasing the frame's responsiveness to excitations that could potentially impact its performance.

The combined results from these tests contributed to a comprehensive understanding of the frame's response to various vibrational inputs. They not only confirmed the absence of significant background vibrations but also laid the groundwork for identifying potential areas for improvement in damping characteristics if required. The insights gained from these tests were instrumental in optimizing the frame's performance and ensuring its suitability for operational environments. Further details and analyses of these tests are discussed in subsequent sections

3.5 IMPACT INPUTS

The selection of impact testing for the initial testing phase was based on its ability to swiftly identify the natural frequencies of the assembled frames, alongside being a common form of induced vibration expected during operational use post-installation. Impact testing involves striking a target and monitoring the subsequent reactions, with a primary focus on assessing the peaks in the frequency domain and damping coefficient from rate of dissapation, crucial parameters for the frames' dynamic behavior. Unlike other applications of impact testing that primarily focus on deformation, the emphasis here is on understanding vibration characteristics rather than structural changes, given the frames' anticipated low deformation environment.

In this testing approach, sensors play a pivotal role in capturing the responses generated by the impact. The analysis revolves around identifying the ringing frequencies produced by the impact and observing the time it takes for these frequencies to decay to the level of random noise. The natural frequency is of paramount importance, aligning with the specified requirement for the warm unit frames to operate outside the 0-15 Hz range and avoid frequencies near multiples of 60 Hz. This criterion is motivated by the need to prevent induced oscillations stemming from environmental factors, such as background vibrations below 15 Hz and electrical grid frequencies at 60 Hz.

Additionally, the damping coefficient, representing the rate at which impact vibrations dissipate over time, is a key metric assessed during impact testing. If the frames are stiff the k would be quite high but since the rate that g decays was less, then 0.1 second as seen in Figure 30 this also implies a large damping coefficient.

The impact vibrational testing phase involved a strategic selection of multiple impact locations and directions to comprehensively evaluate the vibrational behavior of the system. For a robust data collection process, each strike location and position underwent a minimum of three repeated strikes, following the guidelines outlined in [12-15]. Additional strikes were performed whenever necessary to ensure a statistically significant dataset. Throughout the testing phase, two additional positions were identified to encompass not only various levels of the frame but also different impact orientations on the frame structure. This approach facilitated a comprehensive review encompassing various system extremities and dynamics, aiming to understand the impact at specific points within the system.

The selection of these strike locations was crucial as it allowed for the assessment of individual subsystems' impacts on the overall system. Specifically, it provided insights into the

effects on different components such as the magnet and various sections like the middle or top of the HB-650 Warm Unit frame, as well as the base and top of the HB-325 Warm Unit frame. This detailed analysis helped in understanding how vibrations propagate within the system and how different components contribute to overall system dynamics.

Furthermore, considering the impact direction in the testing protocol added another layer of evaluation. While correlations between impact direction and system response were not assumed based on prior modeling, exploring this aspect provided valuable insights into any potential directional influences on vibrations. The strike list, as depicted in Figure 36, exemplifies the systematic approach taken to conduct these impact tests, ensuring a comprehensive assessment of the system's vibrational characteristics under varying conditions.

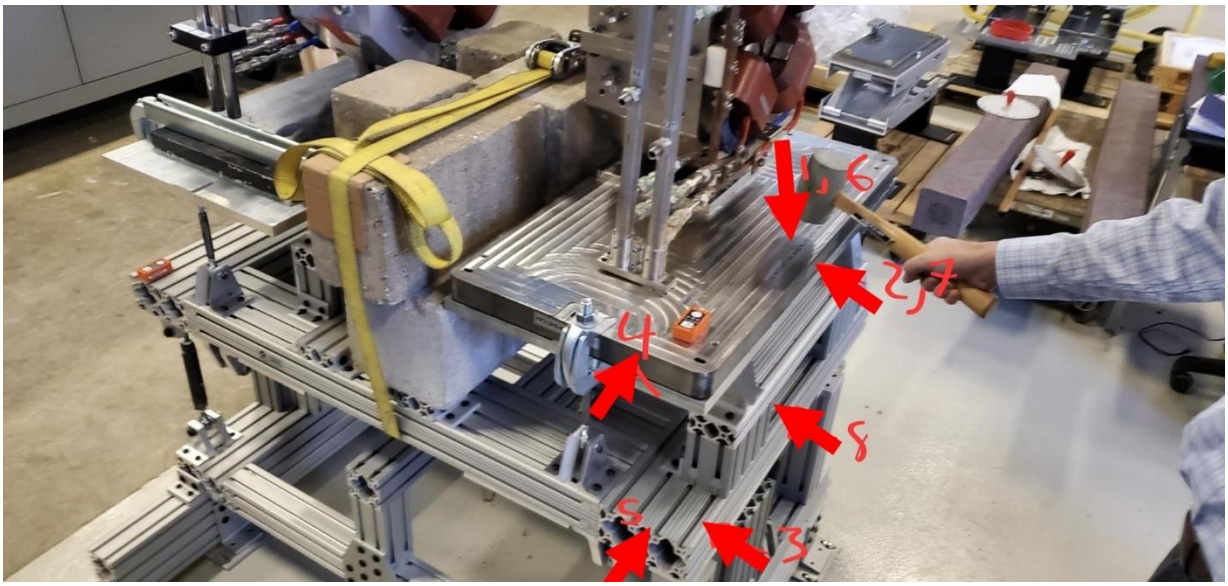

Figure 36: HB-650 Warm Unit frame with marks showing where impacts will be performed

The primary observation derived from the impact vibrational testing centers on the rapid dissipation of ringing frequencies, which exhibited a remarkable decay within a fraction of a second, as visually represented in Figure 30. Another critical insight gained from these tests was

the determination that the damping coefficient must be quite large, highlighting the inherent damping characteristics of the system. This outcome underscores the system's proficiency in mitigating vibrations effectively, a pivotal aspect for evaluating its dynamic behavior and overall structural robustness.

Of significant note, the impact testing did not reveal a discernible natural frequency, as evident from the graph in Figure 37, where no prominent peaks were observed over a average of over 10 samples each with at least three strikes per sample.

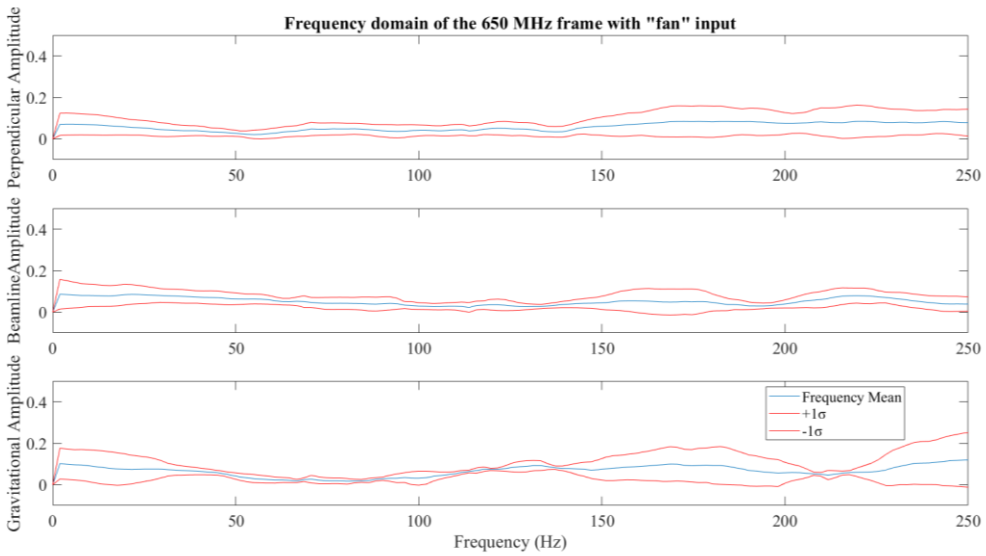

Figure 37: Averaged frequency domain plot of an impact on the fully loaded HB-650 Warm Unit frame

This absence suggests that either the natural frequency falls beyond the detection range of the sensors (0-250 Hz) or there may be operational issues with the sensors themselves. The more likely cause points to a high natural frequency, consistent with the findings from the modeling phase [5]. However, to validate sensor sensitivity and confirm the ability to detect vibrations through the Warm Unit frames, an induced oscillation at a known frequency was subsequently conducted, a detailed account of which will be provided in the subsequent section.

In summary, the impact vibrational testing strategy was designed to provide a comprehensive insight into the system's dynamic response, encompassing various impact scenarios and directions. This approach aimed to uncover subtle variations in vibrational behavior across the warm unit frames and associated components, contributing to a thorough understanding of the system's overall performance under dynamic loading conditions.

3.6 OSCILLATION INPUTS

Apart from impact testing, oscillation vibrational testing emerged as an essential phase in the testing protocol. This decision stemmed from two disparate parts, first the needed confirmation of sensors being able to detect vibrations acting through the Warm Unit frames and secondly, the recognition that while prolonged exposure to direct vibrations is improbable, the frames must still effectively dampen frequencies to prevent potential damage to critical magnet systems. Two distinct tests were conducted: a series of fan tests and a set of more robust push tests.

3.6.1 FAN TESTS

As previously mentioned, the primary objective of the fan test was to assess the sensors' capability to detect vibrations through the frame and to evaluate the uniformity of node transfer. To achieve this, a sensor was directly connected to the fan, while regular sensors were employed to detect vibrations within the frame. In order to induce vibrations at a frequency close to one of the known modes of the frame, a desk fan was adapted by adding an uneven weight to one of its blades, as illustrated in Figure 38.

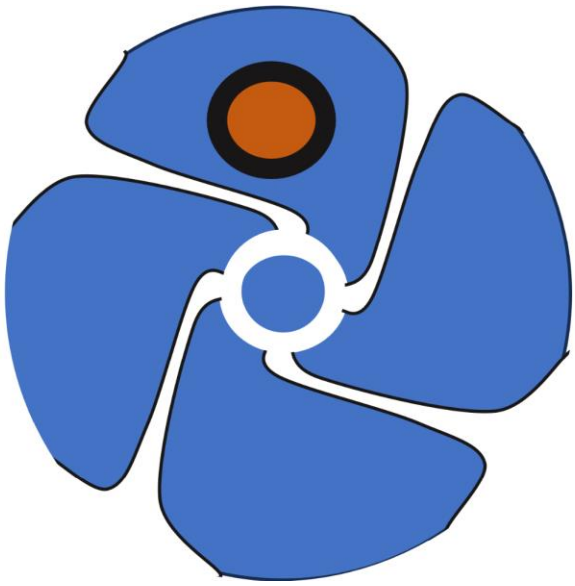

Figure 38: A schematic of the modified fan with an added weight to one of the blades.

Due to the imbalance of weight but consistent rotation rate, the input amplitude could be increased and the frequency of the fan could be better highlighted. the frequency of the fan was selected to be a frequency close to the one outlined as mode 2 in Table 2. This newly achieved frequency was measured and determined to be approximately 29 Hz.

These oscillations were directly monitored by a sensor connected to the fan itself, along with three sensors positioned at extremities distant from the fan, and one sensor placed on the magnet to observe the propagation of vibrations through the turnbuckles. The fan generating these oscillations was affixed to the base layer, as it is anticipated that this layer would bear the brunt of such vibrational loads originating from an external source, given that there should be no other connection points to the frame beyond its contact with the ground.

The sensor directly connected to the fan provided promising results, seen in Figure 39. the analysis script limited its number of points of interest to the first 2^11 data in the time domain. this was then analyzed as discussed above to yield the results seen in Figure 39, which

shoe a large peak at the input frequency. Subsequent values above the noise are at n-multiples of the 29 Hz.

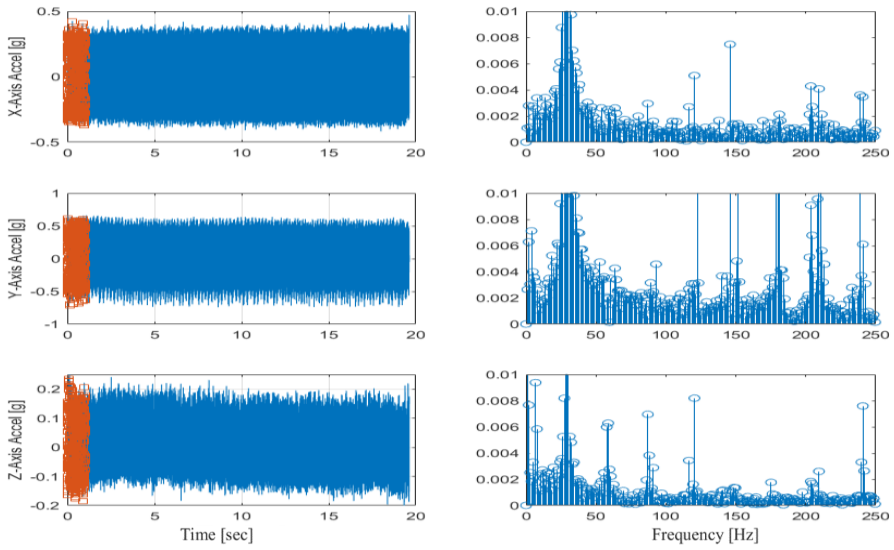

Figure 39: Graphs showing the acceleration over time (left column) and frequency domain (right column) for of a sensor connected to the fan for the, perpendicular (top row), beamline (center row) and, gravitational (bottom row) directions

Subsequently, data from the extremities sensors was gathered and extracted for analysis using the methodology previously outlined, resulting in the generation of an average frequency plot depicted in Figure 40.

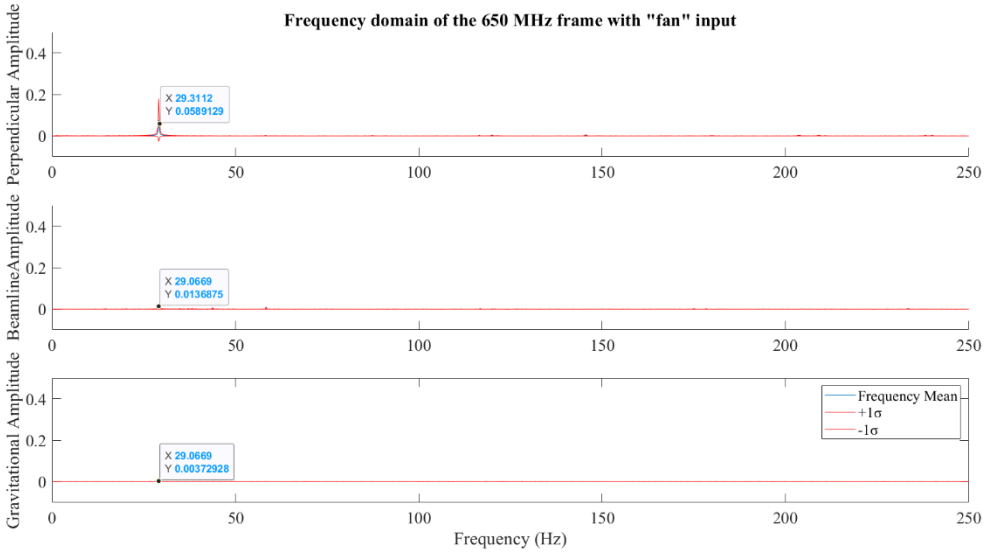

Figure 40: Averaged frequency domain plot of induced vibration of 29Hz. on the fully loaded HB-325 Warm Unit frame

Once more, the outcomes of this phase of testing exhibited encouraging findings, indicating a nearly consistent transmission of frequency across the entirety of the frame structure. This consistent frequency transfer of 29Hz. even at extremely small amplitudes is an important indicator of the frame's ability to effectively distribute and manage oscillations, as expected from the simulated results.

The experimental procedure was repeated by incorporating dummy weights to mimic a load equivalent to 1.5 times the expected operational load of the frames. This decision stemmed from the hypothesis that increased load would result in heightened damping within the system. However, upon thorough analysis, no significant variance was observed. This lack of noticeable difference suggests that there was no substantial systematic alteration in the resonant frequencies of the Warm Unit frames, at least not within the measured parameters of concern to Fermi National Laboratory. This insight provides valuable information regarding the structural stability and resilience of the frames under varying load conditions.

The comprehensive examination through fan oscillation tests revealed essential insights into the vibrational behavior of the frame under low-energy, low-frequency conditions. Surprisingly, the tests indicated that even when the oscillations were set near resonant frequencies, the frame remained unexcited. This resistance to excitation can be attributed to the substantial damping present within the assembly, showcasing its effectiveness in mitigating vibrations even at low energy levels.

Furthermore, these tests provided confirmation that the sensors effectively detected vibrations propagating through the frame. This detection capability strongly implies that the natural frequency of the frame resides above the range of concern suggested in the impact testing results. This aligns with expectations and adds another layer of assurance regarding the structural

integrity and vibrational stability of the Warm Unit frames, especially in environments where low-energy oscillations might be present.

3.6.2 PUSH TESTS

In addition to the low energy oscillations created by a fan a more extreme oscillation test was desired as it was possible that the frame could undergo extreme levels of vibration in some of the worst-case scenarios. To test these higher energy oscillations hey technician hold on to the top plate as well as to a sensor and vigorously shook the top plate back and forth for a period of about 1 second before allowing the frame to reset to normal then repeating that push another two times, as seen in Figure 41. This test was repeated in two directions, In the beamline direction and in the direction perpendicular to the beam line, and at two locations, at the upstream top plate and at the downstream top plate.

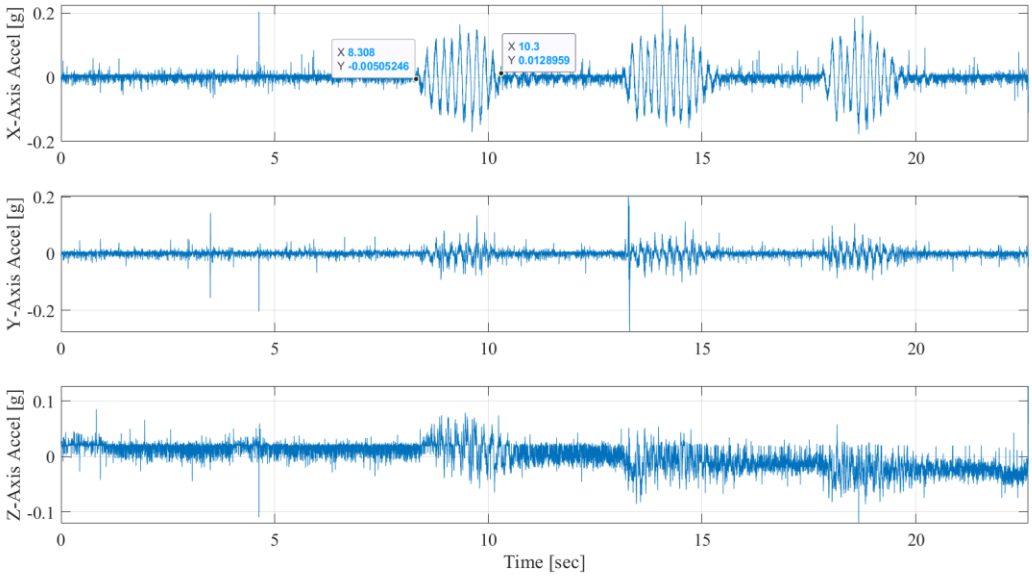

Figure 41: Plot of push test with three pushes

As with the fan test a sensor was connected to the inputting oscillation in this case held by technician as well as 3 sensors on the extremities of the HB-650 Warm Unit frame as well as an additional one on the corrector magnet as this is the location of greatest concern.

It is important to note that while the system did take longer for the vibrations to decay it still was able to decay to background levels relatively quickly (within 2 seconds) as can be seen in Figure 41 above. Similar to the fan test the vibrations were shown to uniformly propagate through the frame as shown in Figure 42.

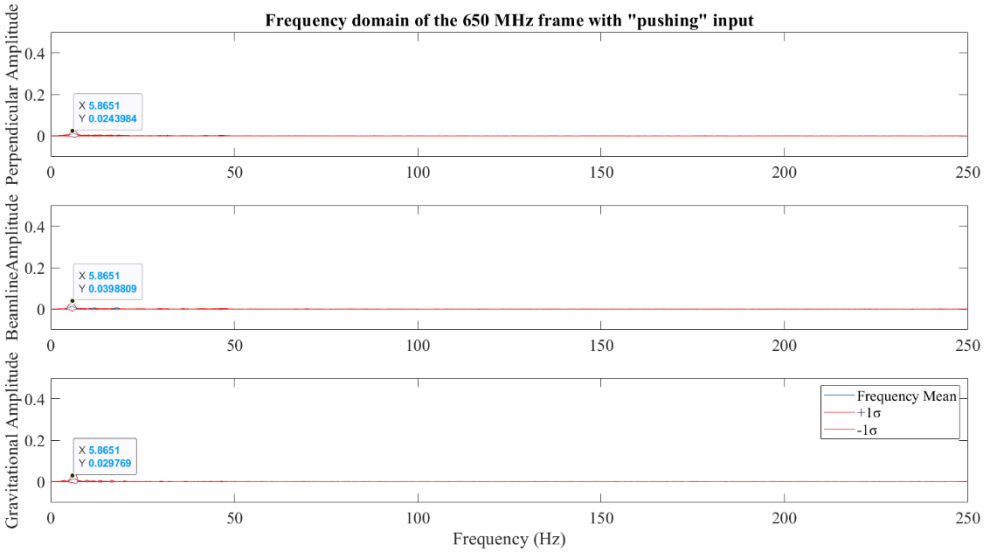

Figure 42: Averaged frequency domain plot of high energy induced vibration on the fully loaded HB-650 Warm Unit frame

This confirms the finding in the low energy oscillation tests of the fan tests as well as providing additional assurance that in the worst-case scenario of heavy equipment running down the tunnel close enough to the frame to excite it or possible seismic activity that other systems would be damaged before the HB-650 Warm Unit frame meaning this frame would not be a point of failure.

3.7 VIBRATIONAL TESTING SUMMARY

Multiple input types were tested into the frame through many repeated experiments. each test built on top of each other in order to strongly prove that the frames did not exhibit a resonance response. This was able to satisfy the need for the frames to be outside of the 0-15 Hz. frequency ranges therefore satisfying the modal needs. The testing below covers the required range of motion to ensure the frames are able to meet the requirements while still not experiencing major adjustments to their resonance frequencies.

4. DISPLACEMENT TESTING

Further tests were deemed necessary to explore avenues for enhancing installation efficiency. Among these tests, one focused on confirming the frictional characteristics during the push test, particularly concerning the sliding action on the fast plates. Another crucial test involved assessing the length variations of the turnbuckles, investigating their extension and contraction effects on the available rotation space.

In conducting the rotation space confirmation test, the primary objective was to demonstrate the linearity of the system. This demonstration aimed to establish that adjustments to a single turnbuckle did not significantly impact the angle of the top layer beyond the desired, pitch, roll or, yaw change. This test was vital in ensuring the precise control and predictable behavior of the turnbuckles in maneuvering the Warm Unit frames during subsequent operation. Through these displacement tests, valuable insights were gained to inform potential refinements and optimizations in the installation process, contributing to the overall effectiveness and reliability of the system.

4.1 OVERVIEW

The displacement testing involved a series of strategic steps to evaluate the practicality and efficiency of the installation process. Firstly, to facilitate these tests, bolt holes were drilled into the concrete floor of A0, providing a stable foundation for subsequent evaluations. This setup simulated the environment expected in the final location of the Warm Unit frames.

The testing apparatus included two 8020 corner brackets securely affixed to the floor, positioned to serve as anchoring points for a hydraulic jack. This arrangement, as depicted in Figure 43, allowed the hydraulic jack to exert controlled pressure during the testing procedures.

The objective was to simulate realistic installation conditions and assess how the system responded under specific loads and orientations.

Figure 43: Test setup for the C channel slide test

The hydraulic jacks were then connected to a fluid system and carefully engaged to apply gradual pressure, simulating the installation force expected during the actual assembly process. The fully loaded HB-650 Warm Unit frame with, two prototype magnets from BARC and 80 kg blocks to represent instrumentation and vacuum pump loads were mounted on to the frame representative of real-world conditions, was subjected to controlled displacement out of the C channel. This displacement mimicked the movements necessary for proper installation and alignment within the designated space.

Additionally, the orientation of the fully loaded HB-650 Warm Unit frame was deliberately rotated to deviate from its initial straight alignment within the C channels. This intentional misalignment was a crucial aspect of the testing process, aiming to evaluate the system's adaptability and ease of installation even under less-than-ideal conditions.

The primary focus of these displacement tests was to validate that even under varied orientations and loading scenarios, the Warm Unit frame could still be easily installed into its

designated final location. By systematically evaluating these parameters, the testing provided valuable insights into potential challenges and opportunities for optimization, ultimately contributing to a more robust and streamlined installation process.

In addition to the C-channel push tests the maximum extension and retraction of the turnbuckles also had to be tested. This was done in accordance with recommendations outlined in [6], an investigative process was undertaken involving the extension of turnbuckles by one rotation, followed by a recording of the angle of the top layer relative to the direction perpendicular to the beamline and the direction of the beamline. This procedure aimed to comprehensively assess the maneuverability and positional stability of the top plates, which hold critical diagnostic equipment essential for maintaining alignment and facilitating maintenance tasks in alignment with the overarching mission objectives of PIP-II.

To achieve a holistic perspective, the procedure was repeated by adjusting the opposing side of the turnbuckle as outlined in previous studies. This iterative process allowed for a comparative analysis of angle variations, providing insights into the symmetry and balance of adjustments across the frames.

The underlying goal of this testing regimen was to validate and optimize the maneuverability of the top plates, which play a pivotal role in supporting diagnostic instruments and ensuring alignment integrity critical to the operational success of the PIP-II mission. By systematically evaluating the effects of turnbuckle adjustments on angle changes in the top layer, the testing sought to identify any potential constraints or limitations in the assembly's maneuvering capabilities. Such insights are invaluable for refining assembly protocols and enhancing the overall functionality and reliability of the Warm Unit frames within the operational context of PIP-II.

4.2 C CHANNEL SLIDING CONFIRMATION

Multiple push tests were conducted in order to confirm that the frames would be able to be easily installed into their final locations. To test this to hydraulic jacks or pressed against the base of the HB-650 Warm Unit frame and extended in tandem such that the HB-650 Warm Unit frame would move smoothly on the breath please. The hydraulic jacks or brace against a 2020 8020 bracket which is affixed to the floor in line with the 2 space legs of the HB-650 Warm Unit frame as can be seen in FIG.

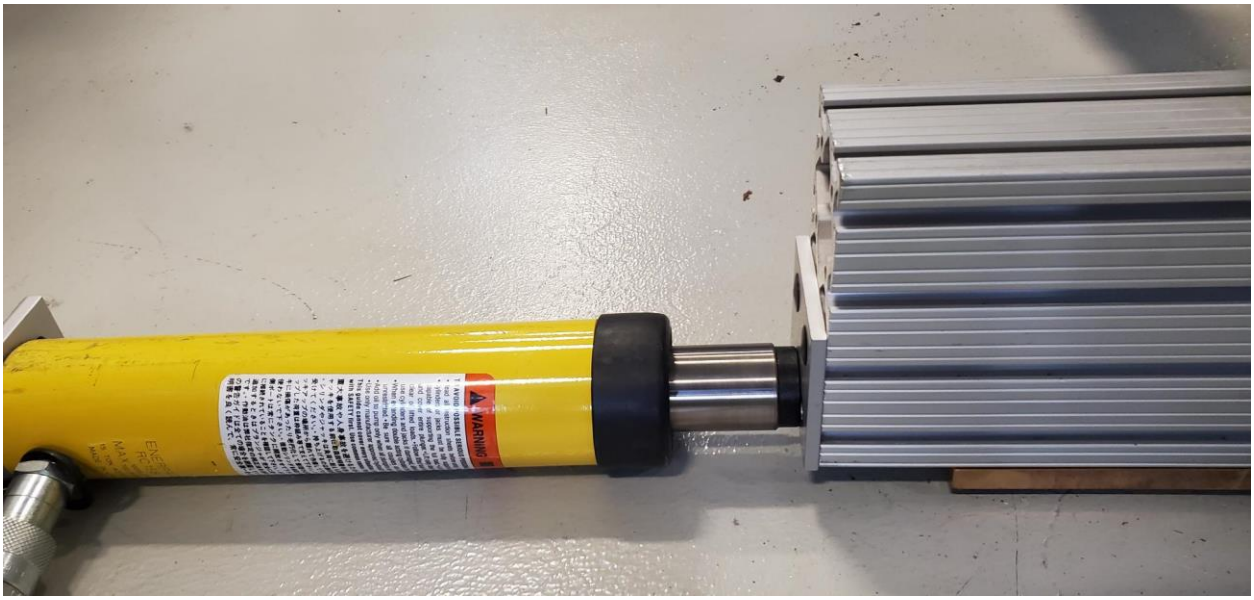

Figure 44: Test setup for the C channel slide test with the jack engaged and pushing on one of the 650 legs

The first rest had two technicians pumping in tandem. This resulted in the base layer of the fully loaded HB-650 Warm Unit frame moving smoothly over the brass plates and were able to maintain the alignment that was originally set. A follow up test was also conducted to determine if the frame could also be installed the frame started when the frame started out of alignment this was done by preemptively using only one of the jacks to extend into the HB-650 Warm Unit frame such that when they followed the steps outlined in the first test of the

installation that the HB-650 Warm Unit frame would not glide parallel to the C channels anchored to the floor but would instead go at some angle to them. To ensure that the installation could go smoothly even with one technician a test was done where only one of the jack were engaged at one time. This was done to simulate a technician moving between the two jacks and alternating the leg that received the “pushes”. All of the tests outlined above were able to successfully both push the frame into and out of the beamline position.

4.3 ROTATION SPACE CONFIRMATION

A confirmation of the full maneuverability was tested. This was done by turning specific turnbuckles while keeping others stationary or turning them in the opposite direction this would give resulting frames as seen in Figure 45. The measurement of each full rotation of a large turn buckle produces a displacement of 2.54mm. This requires the ability to be able to turn the large turnbuckles 12 times to achieve the necessary positional adjustment.

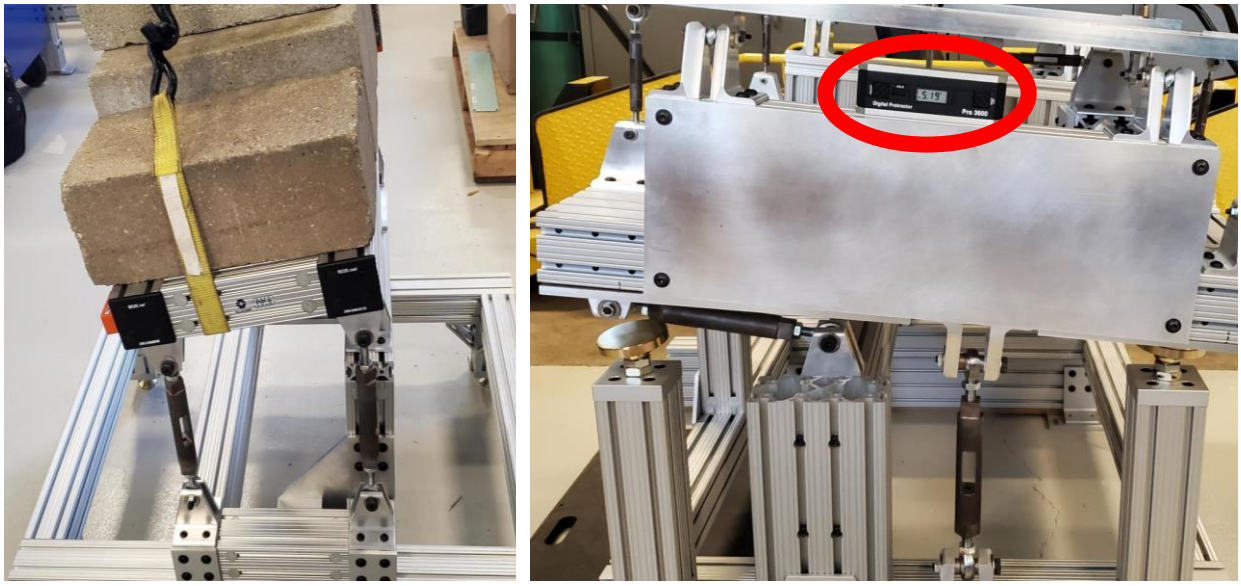

Figure 45: Turnbuckle adjustability test of the HB-325 Warm Unit frame (left) and HB-650 Warm Unit frame (right)

Depending on the desired result the technician can rotate the turnbuckles individually or in tandem. This will also adjust the position of the top plate unless cancelled out by rotations in

other turnbuckles on the frame. A 2D example of the possible nonlinearity can be seen in Figure 46 where the lengths of rods A and B are fixed but rod C is allowed to extend.

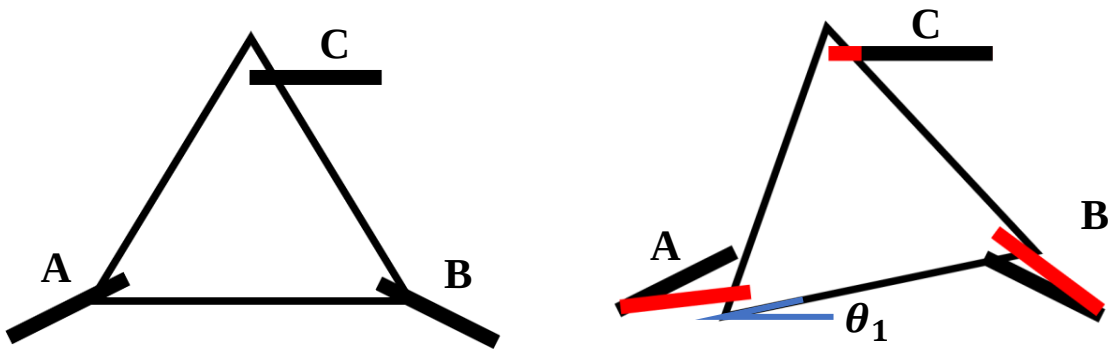

Figure 46: A 2D representation of a plate being adjusted by lengthening one rod while two other rods connected at pin joints are kept at a certain length.

To avoid the effects of this nonlinearity from moving the magnets and diagnostic equipment off beamline the wheelbase can be made larger as illustrated in Figure 47 where the change between θ_1 and θ_2 is directly proportional to the increase of the size of the place from Figure 46 to Figure 47. In both the HB-325 and HB-650 Warm Unit frames the wheelbase is large enough that the top layers are expected to display a relatively strong level of linearity.

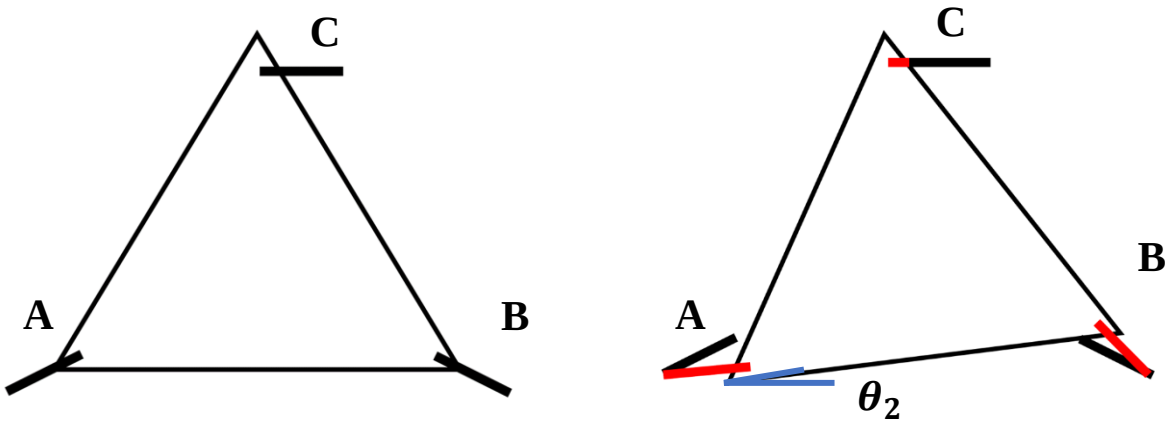

Figure 47: A 2D representation of a larger plate being adjusted by lengthening one rod while two other rods connected at pin joints are kept at a certain length.

The procedure is outlined in previous work without the specifics of how to achieve the desired top plate rotation while keeping the positional piece as constant as possible. In order to

do this one side would be extended while another side contracted with the angle of the top plate of the frame being recorded at each full turn of the turnbuckle. The resulting rotational space of the HB-325 and HB-650 Warm Unit frames can be seen in the Figure 48 below. The rotational space shown below is the result of exploring the entire parameter space to examine the angles achieved while confirming that they are aligning with the requirements of ± 30 mm for the large turnbuckles and ± 15 mm for the large turnbuckles. In order to get the changes in position a digital level was used as seen circled in red in Figure 45. This angle is what is being shown in the color map of Figure 48. It was found through the results seen below that there is linearity of the adjustment without the full need of all six turn buckles. The additional turnbuckles do however allow for further adjustment in space as well as increasing the linearity of adjustment when utilized.

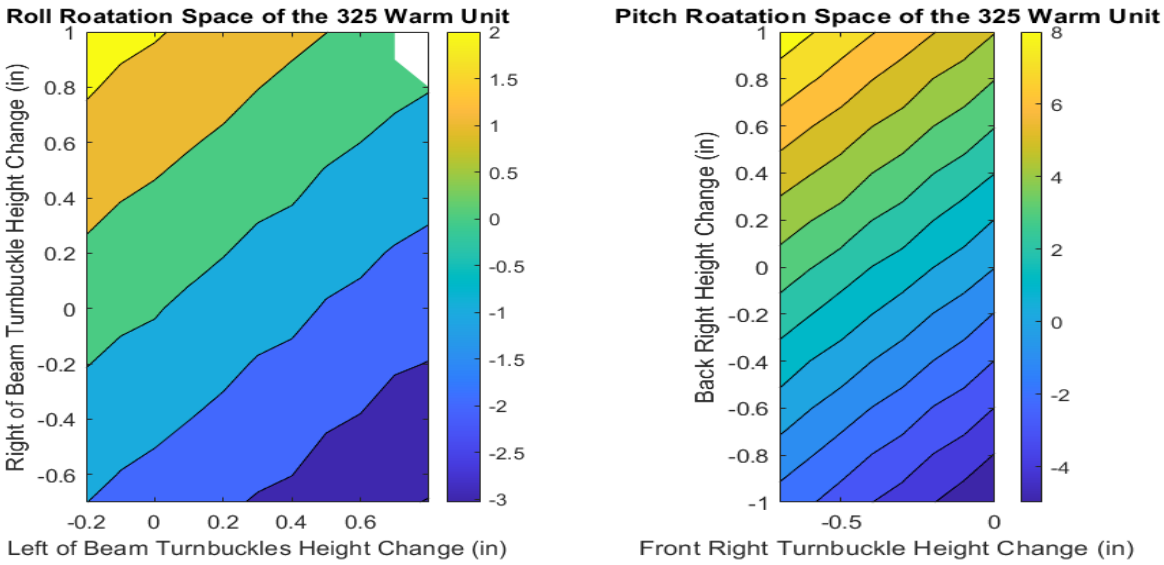

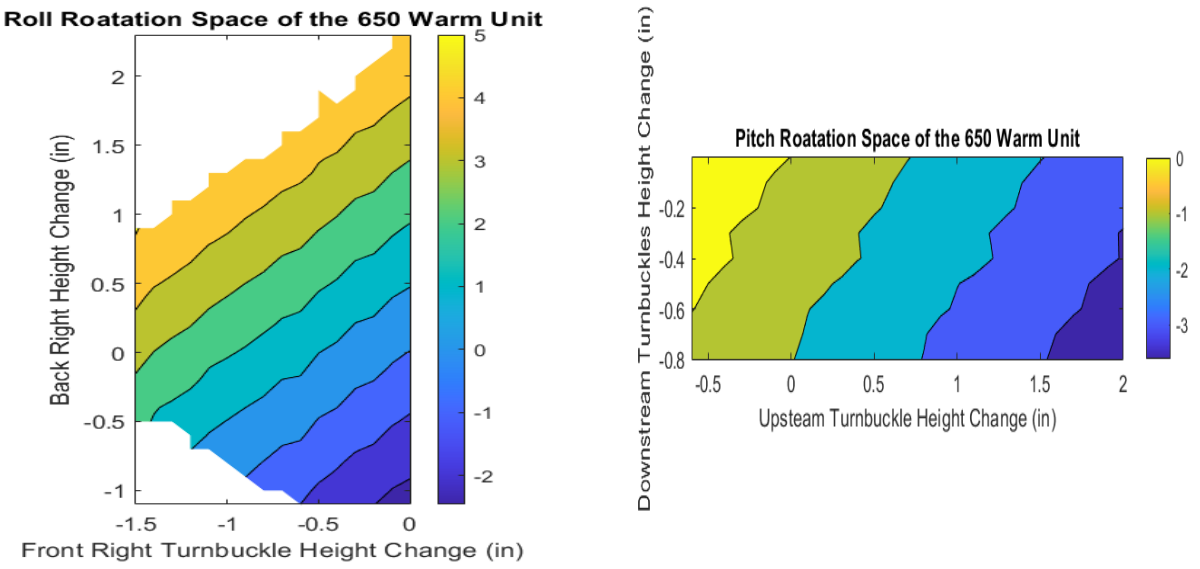

Figure 48: Contour plots displaying to measured rotation space in Roll (left column) and Pitch (right column) for the HB-325 Warm Unit frame (top row) and HB-650 Warm Unit frame (bottom row)

5. CONCLUSION

The successful assembly of the frames represents a significant milestone in this engineering endeavor that move beyond simulation analysis in 3D modeling software [5, 6]. Through rigorous testing and evaluation, it has become evident that the frames exhibit robust performance characteristics, requiring only minor adjustments during subsequent procurement and production phases. Notably, the frames demonstrate exceptional damping capabilities, effectively attenuating vibrations and exhibiting resonance frequencies well beyond the range of concern identified by Fermi National Laboratory.

One of the key findings of this study is the frames' remarkable maneuverability, showcasing their adaptability during installation processes. The ample rotation space available in the upper layer allows for seamless adjustments to accommodate various flooring configurations, ensuring optimal positioning and alignment in diverse operational environments.

These outcomes underscore the reliability and functionality of the frames, highlighting their suitability for deployment in critical applications. The comprehensive testing regimen has provided valuable insights into the frames' dynamic behavior, confirming their structural integrity and operational effectiveness. Moving forward, the identified minor adjustments will be addressed to further enhance the frames' performance and streamline their production processes.

In conclusion, the successful assembly, coupled with robust testing results, positions the frames as resilient and versatile components capable of meeting the stringent requirements of Fermi National Laboratory.

5.1 OVERVIEW

The completion of several critical components has been successfully confirmed during the project. Firstly, the translation of struts through full extension and retraction was verified,

both independently and in conjunction. Additionally, the positioning and rotational limits of the upper magnet support and the entire raft were determined and validated. Furthermore, it was demonstrated that the fully loaded HB-650 Warm Unit frame maintains three-point contacts with the rails as required. Both frames exhibited operational capabilities consistent with expectations, even when subjected to loads exceeding the anticipated levels by 50%. To quantify the resonance frequencies of the structure accurately, vibration tests were conducted using impact hammers and induced oscillations. These tests provided valuable insights into the structural dynamics and performance characteristics of the frames under various conditions.

5.2 DATA VALIDATION

Of significant note, the impact testing did not reveal a discernible natural frequency, as evident from the graph in Figure 37, where no prominent peaks were observed. This result in conjunction with the vibrational response seen in Figure 40 implies that the natural frequency falls beyond the detection range of the sensors (0-250 Hz). This is consistent with simulations done previously in [6].

The results in Figure 40 indicate that even when the oscillations were set near resonant frequencies, the frame remained unexcited. This resistance to excitation can be attributed to the substantial damping present within the assembly. This aligns with expectations and adds another layer of assurance regarding the structural integrity and vibrational stability of the Warm Unit frames, especially in environments where low-energy oscillations might be present.
As shown by Figure 41-42 the frame was able to uniformly transfer vibrations further confirming the assumptions found above even in the presence of high energy oscillations.

5.3 NEXT STEPS

Several key improvements and adjustments have been identified based on the assembly and testing processes conducted. First, modifications to the turnbuckles have been recommended and incorporated into the assembly and procurement instructions. Specifically, enhancing the tolerancing for the ball rod ends to reduce play was ultimately selected.

Furthermore, a shadow box design is in progress to streamline the turnbuckle assembly process, with precise thread depth settings tailored for technicians. An unnecessary plate, as highlighted in Figure 26, has been removed from the assembly instructions and orders. This adjustment not only reduces costs but also simplifies the assembly process.

Another crucial improvement involves decreasing the size of the through hole of the turnbuckle mounting brackets, as illustrated in Figure 27. The current size of the through hole was deemed too large.

Finally the full installation and assembly of the 13 frames still needs to be undertaken however it was estimated that once started this could be finished within 6 months by an experienced technician.

REFERENCES

[1] Proton Improvement Project II: Preliminary Design Report. J. Adetunji, 'et al'. J. Anderson, R. Andrews, C. Baffes, M. Ball, T. Banaszkiewicz, S. Belomestnykh, … R. Zifko. Argonne National Laboratory, Lemont, IL 60538, USA. Bhabha Atomic Research Center, Mumbai, India. Fermi National Accelerator Laboratory, Batavia, IL 60510, USA. Raja Rammana Center for Advanced Technology, Indore, India. Wroclaw University of Science and Technology, Wroclaw, Poland

[2] ORCA Stand Design for PIP-II Cryomodules: Introduction and Charge. C. Baffes.PIP-II Cryomodule Stand Preliminary Design Review. Nov 7, 2018

[3] ORCA Stand Design for PIP-II Cryomodules: Design Overview. J. Batko. PIP-II Cryomodule Stand Preliminary Design Review. Nov 7, 2018

[4] ORCA Stand Design for PIP-II Cryomodules: Analysis. J. Batko. PIP-II Cryomodule Stand Preliminary Design Review. Nov 7, 2018

[5] WARM UNIT ROD MOVEMENT STAND FOR PROTON IMPROVEMENT PROJECT II. C. Becker (2021)

[6] WARM UNIT STAND ANALYSIS FOR PROTON IMPROVEMENT PROJECT II M. Pavlick (2022)

[7] Custom Aluminum Framing Systems Product Catalog 24. 80/20 https://downloads.8020.net/downloads/misc/download/id/374 . Mar 24 2024

[8] PIP-II Warm Unit Structures Technical Requirements Specification. ED0008578. C. Baffes, N. Pohlman (2020)

[9] FESHM 5100: Structural Safety. B. Rubik, M. White. Fermilab Environment Safety and Hazards Manual.
Revised Sept 2020

[10] Minimum Design Loads for Buildings and Other Structures. ASCE Standard ASCE/SEI 7-10. American
Society of Civil Engineers

[11] Aluminum Design Manual. The Aluminum Association. Copyright 2010

[12] Measurement and Data Analysis for Engineering and Science: 3rd Edition. P. F. Dunn. CRC Press. 2011

[13] Design and Analysis of Experiments: 7th Edition. D. C. Montgomery. Wiley (2008)

[14] The Design of Experiments: Oliver and Boyd. R. A. Fisher (1935)

[15] An Introduction to Design of Experiments: A Simplified Approach. L. B. Barrentine. ASQ Quality Press (1999)

[16] enDAQ, “S4 Vibration Sensor,” S4-D40 datasheet, 2024